





RESEARCH ARTICLE

Increased expression of the ATP-gated P2X7 receptor reduces responsiveness to anti-convulsants during status epilepticus in mice

Edward Beamer^{1,2} | James Morgan^{1,3} | Mariana Alves¹ |
 Aida Menéndez Méndez¹ | Gareth Morris^{1,4} | Béla Zimmer⁵ | Giorgia Conte¹ |
 Laura de Diego-García¹ | Cristina Alarcón-Vila⁶ | Nico Ka Yiu Ng¹ |
 Stephen Madden⁷ | Francesco Calzaferrì⁸  | Cristóbal de los Ríos^{8,9} |
 Antonio G. García^{8,9} | Michael Hamacher¹⁰ | Klaus Dinkel¹¹ |
 Pablo Pelegrín^{6,12}  | David C. Henshall^{1,4} | Annette Nicke⁵  | Tobias Engel^{1,4} 

¹Department of Physiology and Medical Physics, RCSI University of Medicine and Health Sciences, Dublin, Ireland

²School of Science and Technology, Nottingham Trent University, Nottingham, UK

³Division of Developmental Biology and Medicine, School of Medical Sciences, Faculty of Biology, Medicine and Health, University of Manchester, Manchester, UK

⁴FutureNeuro, SFI Research Centre for Chronic and Rare Neurological Diseases, RCSI University of Medicine and Health Sciences, Dublin, Ireland

⁵Walther Straub Institute of Pharmacology and Toxicology, Faculty of Medicine, Ludwig-Maximilians-Universität München, Munich, Germany

⁶Instituto Murciano de Investigación Biosanitaria (IMIB-Arrixaca), Hospital Clínico Universitario Virgen de la Arrixaca, Murcia, Spain

⁷Data Science Centre, RCSI University of Medicine and Health Sciences, Dublin, Ireland

⁸Instituto-Fundación Teófilo Hernando and Departamento de Farmacología, Facultad de Medicina, Universidad Autónoma de Madrid, Madrid, Spain

⁹Instituto de Investigación Sanitaria, Hospital Universitario de La Princesa, Madrid, Spain

¹⁰Affectis Pharmaceuticals AG, Dortmund, Germany

¹¹Lead Discovery Center GmbH, Dortmund, Germany

¹²Department of Biochemistry and Molecular Biology B and Immunology, University of Murcia, Murcia, Spain

Correspondence

Tobias Engel, Department of Physiology and Medical Physics, Royal College of Surgeons in Ireland, University of Medicine and Health Sciences, Dublin D02 YN77, Ireland.
 Email: tengel@rcsi.ie

Funding information

European Research Council, Grant/Award Numbers: 899636, 614578; Fundación Séneca, Grant/Award Numbers: 21081/PDC/19, 20859/PI/18; FEDER/Ministerio de Ciencia, Innovación y Universidades - Agencia Estatal de Investigación, Grant/Award Numbers: PID2020-116709RB-I00, SAF2017-88276-R; Deutsche Forschungsgemeinschaft, Grant/Award Number: SFB 1328 (P15); Irish Research Council, Grant/Award Numbers:

Background and Purpose: Refractory status epilepticus is a clinical emergency associated with high mortality and morbidity. Increasing evidence suggests neuroinflammation contributes to the development of drug-refractoriness during status epilepticus. Here, we have determined the contribution of the ATP-gated P2X7 receptor, previously linked to inflammation and increased hyperexcitability, to drug-refractory status epilepticus and its therapeutic potential.

Experimental Approach: Status epilepticus was induced via a unilateral microinjection of kainic acid into the amygdala in adult mice. Severity of status epilepticus was compared in animals with overexpressing or knock-out of the P2X7 receptor, after inflammatory priming by pre-injection of bacterial lipopolysaccharide (LPS) and in mice treated with P2X7 receptor-targeting and anti-inflammatory drugs.

Abbreviations: ASD, anti-seizure drugs; EGFP, enhanced green fluorescent protein; KA, kainic acid; LPS, lipopolysaccharide; P2X7R-OE, P2X7 receptor overexpression; RSE, refractory status epilepticus; WT, wild-type.

Edward Beamer, James Morgan and Mariana Alves contributed equally.

Aida Menéndez Méndez and Gareth Morris contributed equally.

GOIPD/2020/806, GOIPD/2020/865; H2020 Marie Skłodowska-Curie Actions Individual Fellowship, Grant/Award Numbers: 840262, 796600, 884956, 753527; Marie Skłodowska-Curie, Grant/Award Number: 766124; Science Foundation Ireland, Grant/Award Numbers: 16/RC/3948, 17/CDA/4708, 13/SIRG/2098; Health Research Board, Grant/Award Number: HRA-POR-2015-1243

Key Results: Mice overexpressing P2X7 receptors were unresponsive to several anti-convulsants (lorazepam, midazolam, phenytoin and carbamazepine) during status epilepticus. P2X7 receptor expression increased in microglia during status epilepticus, at times when responses to anticonvulsants were reduced. Overexpression of P2X7 receptors induced a pro-inflammatory phenotype in microglia during status epilepticus and the anti-inflammatory drug minocycline restored normal responses to anticonvulsants in mice overexpressing P2X7 receptors. Pretreatment of wild-type mice with LPS increased P2X7 receptor levels in the brain and reduced responsiveness to anticonvulsants during status epilepticus, which was overcome by either genetic deletion of P2X7 receptors or treatment with the P2X7 receptor antagonists, AFC-5128 or ITH15004.

Conclusion and Implications: Our results demonstrate that P2X7 receptor-induced pro-inflammatory effects contribute to resistance to pharmacotherapy during status epilepticus. Therapies targeting P2X7 receptors could be novel adjunctive treatments for drug-refractory status epilepticus.

KEYWORDS

drug-refractoriness, inflammation, mouse models, P2X7 receptor, status epilepticus

1 | INTRODUCTION

Status epilepticus, defined as a prolonged seizure lasting more than 5 min or two or more isolated seizures without full recovery in between, is thought to result from a failure of intrinsic mechanisms to terminate a seizure. The incidence is 10–40/100,000, making this condition one of the most common life-threatening neurological emergencies (Betjemann & Lowenstein, 2015; Sanchez & Rincon, 2016). Status epilepticus is associated with high acute mortality and morbidity and long-term deleterious consequences including an increased risk of developing epilepsy and cognitive decline (Holmes, 2015). The most common causes of status epilepticus are inadequate doses of anticonvulsant drugs in patients with epilepsy, stroke, traumatic brain injury (TBI), toxic-metabolic encephalopathies and neurological and systemic infections (Mayer et al., 2002).

Frontline pharmacotherapy for status epilepticus is primarily via treatment with benzodiazepines, such as **lorazepam** or **diazepam**, followed by anti-seizure drugs (ASDs), such as **phenytoin** or **phenobarbital** (Crawshaw & Cock, 2020). Treatments fail, however, in 31–43% of cases, resulting in refractory status epilepticus (RSE). This is defined as status epilepticus which fails to respond to ≥ 2 ASDs including at least one non-benzodiazepine, with the time spent in status epilepticus increasing the probability of developing drug unresponsiveness. Critically, RSE is linked with a three-fold increase in mortality compared to normal status epilepticus and considerable morbidity (Betjemann & Lowenstein, 2015). The causes and mechanisms of RSE development are incompletely understood, but molecular changes thought to contribute include the internalization of **GABA receptors** and increased surface expression of excitatory **glutamate**

What is already known

- P2X7 receptor expression is increased in the brain after status epilepticus.
- Drugs targeting the P2X7 receptor modulate seizure severity during status epilepticus.

What this study adds

- Elevated P2X7 receptor expression leads to resistance to anticonvulsant drugs.
- ATP-mediated extracellular signalling may contribute to drug refractoriness during status epilepticus.

What is the clinical significance

- The P2X7 receptor contributes to unresponsiveness to anticonvulsant treatments during status epilepticus.
- Blockade of the P2X7 receptor may represent a novel adjunctive therapy for drug-refractory status epilepticus.

(**NMDA and AMPA receptors**) (Betjemann & Lowenstein, 2015). Consequently, there is a pressing need to identify new drug targets that act either independently of GABAergic inhibitory signalling or that can

be given as adjunctive treatment to enhance the effects of current anti-seizure medication.

A role for inflammatory mediators in neuronal function and excitability is well established (Vezzani et al., 2015). Cytokines, such as **IL-1 β** or **TNF- α** , modulate the function of GABA receptors and potentiate excitatory NMDA receptor synaptic transmission, alter voltage-gated ion channel function and expression, and regulate presynaptic exocytosis of both excitatory and inhibitory neurotransmitters (Huang et al., 2010; Rossi et al., 2012; Vezzani & Viviani, 2015). Importantly, several drugs targeting inflammatory signalling pathways have anti-convulsive effects during status epilepticus (Vezzani et al., 2015). An emerging target is the ionotropic, ATP-gated **P2X7 receptor** (Beamer et al., 2021). This ion channel functions as a gatekeeper of inflammation by driving the assembly of the NLRP3 inflammasome and subsequent release of IL-1 β (Di Virgilio et al., 2017). The P2X7 receptor has some unique characteristics that make it particularly attractive: (a) In comparison to other **P2X receptors**, it has a low sensitivity to ATP, suggesting that it is mainly activated under pathological conditions when high volumes of ATP are released, as during a seizure (Beamer et al., 2019). This could spare patients from unwanted side effects during treatment based on P2X7 receptor antagonists. (b) expression of P2X7 receptors increases in the brain following status epilepticus and (c) blockade of the P2X7 receptor with drugs modulates seizure severity and alters the resulting neuropathology in several experimental models of status epilepticus (Beamer et al., 2021; Engel et al., 2012; Jimenez-Pacheco et al., 2013; Jimenez-Pacheco et al., 2016; Kim & Kang, 2011). Whether increased expression or function of the P2X7 receptor contributes to drug-refractoriness during status epilepticus, however, has not been explored to date.

Here, we used a model of focal-onset status epilepticus in mice to determine whether P2X7 receptors contributed to the development of the refractory form of status epilepticus, RSE. Expression of P2X7 receptors was studied by using P2X7 receptor reporter mice and highly specific P2X7 receptor nanobodies (Danquah et al., 2016; Kaczmarek-Hajek et al., 2018). P2X7 receptor function was investigated using a combination of pharmacological and genetic mouse models. We show that drug refractoriness in status epilepticus is, at least in part, mediated via P2X7 receptor-driven inflammation and that inhibition of the receptor can restore responses to current anti-seizure medication.

2 | METHODS

2.1 | Animal models

All animal care and experimental procedures were in accordance with the principles of the European Communities Council Directive (2010/63/EU) and were approved by the Research Ethics Committee of the Royal College of Surgeons in Ireland (RCSI) (REC 1322) and Health Products Regulatory Authority (HPRA) (AE19127/P038; AE19127/P013). The animals were treated according to European standards/regulations for animal experiments, and all efforts were

made to minimize animal suffering and reduce the numbers of animals under experiments. Animal studies are reported in compliance with the ARRIVE guidelines (Percie du Sert et al., 2020) and with the recommendations made by the *British Journal of Pharmacology* (Lilley et al., 2020).

All animals were housed in a controlled biomedical facility using Tecniplast conventional cages (Ref. 1284L EUROSTANDARD TYPE II L) and Lignocel BK8/15-25, premium hygienic animal bedding (D0764P00Z) with two to five mice per cage on a 12-h light/dark cycle at $22 \pm 1^\circ\text{C}$ and humidity of 40–60% with food and water provided ad libitum. For each cage, enrichment was provided in the form of nesting material (irradiated Bed-r'Nest Brown, Datesand, Item code CS1BEB), PVC tubes and red polycarbonate mouse houses. All in vivo studies were carried out during the light phase of the cycle.

All mice used in our experiments were 8–12 weeks old, with a weight range between 25 and 30 g. The following strains and sexes were used: male C57Bl/6 OlaHsd wild-type (WT) mice, obtained from the Biomedical Research Facility at RCSI; heterozygous FVB/N-Tg (RP24-114E20-P2X7/StrepHisEGFP)Ani (line 17) BAC transgenic mice that express the enhanced green fluorescent protein (EGFP) immediately upstream of a *P2rx7* BAC clone over-express P2X7 receptors and are referred to in this paper as P2X7-OE mice (Kaczmarek-Hajek et al., 2018) and the respective WT litter mates (to reduce breeding, we used male and female mice); male C56BL/6N-P2rx7^{tm1d(EUKOMM)wtst} P2X7R knock-out (KO, *P2X7*^{-/-}) mice, obtained from A. Nicke, LMU Munich; and male mice C57BL/6-Nlrp3^{tm1Vmd} KO for NLRP3 (*Nlrp3*^{-/-}), C57BL/6-Pycard^{tm1Vmd} KO for ASC (*Pycard*^{-/-}), B6N.129S2-Casp1^{tm1Flv/J} KO for **caspace-1** and **caspace-11** (*Casp1/11*^{-/-}), obtained from I. Coullin, University of Orleans.

Convulsive status epilepticus in rodents has been used extensively to model seizures and to identify potential novel treatments (Loscher, 2017). Mice are a valuable experimental model of status epilepticus for several reasons including the fact that they share major aspects of brain circuitry with humans, such as the organization and function of the hippocampus. Mice are also large enough to enable multi-channel EEG recordings to score seizures and undergo stereotyped behavioural responses during seizures that have human correlates (e.g., tonic-clonic components). Another reason for using mice is the availability of numerous transgenic lines to study effects of a specific target gene, using P2X7 receptor KO or overexpression (OE).

The exact numbers of mice per experimental group are provided in the respective figure legends. The sample size was calculated using G*Power 3.1.9.4 software with inputs based on data recorded in similar previously performed experiments to determine suitable sample sizes necessary for detecting differences. Inputs for power analyses in these studies were taken from raw data reported in Engel et al. (2012) and Jimenez-Mateos et al. (2012). Student's *t* test: confidence intervals were set at 0.95, giving $\alpha = 0.05$. Power was set at $1 - \beta = 0.8$. The difference between groups ($\mu_1 - \mu_2$) was 35, while standard deviation (σ) was 21. Using these parameters, a group size of 14 was derived.

2.2 | Mouse model of status epilepticus

Status epilepticus was induced as described previously (Alves et al., 2019). Briefly, during stereotaxic procedures, mice were anaesthetised using isoflurane (5% induction, 1–2% maintenance) and maintained normothermic (body temperature was maintained between 36°C and 37°C) by means of a feedback-controlled heat blanket, controlled by a rectal probe (Harvard Apparatus Ltd, Edenbridge, Kent, UK). The depth of the anaesthesia was frequently tested by checking the plantar nociception or corneal reflex. Additionally, to minimize pain during and post-surgery, mice were treated with buprenorphine (0.05 mg·kg⁻¹) and EMLA cream (Aspen Pharma, Maidenhead, UK) which was applied to head wounds and ear bars. Once fully anaesthetised, mice were placed in a stereotaxic frame and a midline scalp incision was performed to expose the skull. A guide cannula (coordinates from Bregma; AP = -0.94 mm, L = -2.85 mm) and three electrodes (Bilaney Consultants, Sevenoaks, UK), one on top of each hippocampus and with the reference on top of the frontal cortex, were fixed in place with dental cement. An Xltek recording system (Optima Medical, Guildford, UK) was used to record electroencephalogram (EEG). Following a recovery period of approximately 1 h post-surgery, status epilepticus was induced via a microinjection of 0.2-μg (FvB/NJ background) or 0.3 μg (C57/Bl6 background) of **kainic acid (KA)** in 0.2 μl phosphate-buffered saline (PBS) into the right basolateral amygdala into awake, hand-restrained mice. Vehicle-injected control animals received 0.2 μl of PBS. The anticonvulsants lorazepam (6 mg·kg⁻¹; Mouri et al., 2008), phenytoin (10 mg·kg⁻¹; Loscher, 2007), carbamazepine (40 mg·kg⁻¹; Twele et al., 2016) or midazolam (8 mg·kg⁻¹; Diviney et al., 2015) were injected i.p., 40 min following intra-amygdala KA at doses previously shown to reduce seizures. EEG was recorded for 10 min before intra-amygdala KA (baseline), during the time of intra-amygdala KA until treatment with anticonvulsant (status epilepticus) and for 60 min post-anticonvulsant treatment (post-status epilepticus). Post-status epilepticus, mice were evaluated using a scoring sheet for scoring endpoints in rodents, approved by the HPRAs, and the mouse Grimace scale. Mice were humanely killed via cervical dislocation by a trained individual, if not otherwise indicated.

2.3 | EEG and behavioural analysis

EEG data were uploaded onto Labchart7 software (AD Instruments), as described earlier (Alves et al., 2019). EEG total power (μV²) is a function of EEG amplitude over time and was analysed by integrating frequency bands from 0 to 100 Hz. Power spectral density heat maps were generated within LabChart7 (spectralview), with the frequency domain filtered from 0 to 40 Hz and the amplitude domain filtered from 0 to 50 mV. Data are presented as *n*-fold to baseline recordings prior to intra-amygdala KA injection, if not indicated otherwise. Behavioural seizures were scored according to a modified Racine Scale, as reported previously (Jimenez-Mateos et al., 2012): score

1, immobility and freezing; score 2, forelimb and or tail extension, rigid posture; score 3, repetitive movements, head bobbing; score 4, rearing and falling; score 5, continuous rearing and falling; score 6, severe tonic-clonic seizures. Mice were scored every 5 min for 40 min after KA injection. The highest score attained during each 5-min period was recorded by an observer, who was blinded to treatment.

2.4 | Drug administration

Minocycline (30 mg·kg⁻¹ in distilled H₂O) was delivered twice via an i.p. injection (200 μl), 4 and 24 h before treatment with intra-amygdala KA (Alves et al., 2019). Lipopolysaccharide (LPS; 1 mg·kg⁻¹ in PBS) was delivered via an i.p. injection (100 μl) 72 h before intra-amygdala KA injection. The NLRP3 inhibitor MCC950 (100 μM in distilled H₂O) or vehicle was delivered via an intracerebroventricular (i.c.v.) injection (2 μl), 40 min post-intra-amygdala KA injection at the time-point of treatment with the anticonvulsant lorazepam. The P2X7 receptor antagonist AFC-5128 (50 mg·kg⁻¹) (Fischer et al., 2016) or vehicle (*N,N*-dimethylacetamide and 45% 2-hydroxypropyl-β-cyclodextrin, in a final ratio of 1:9) were delivered via i.p. (200 μl), 40 min following intra-amygdala KA injection at the time-point of treatment with the anticonvulsant lorazepam. Likewise, the P2X7 receptor antagonist **ITH15004** (Calzaferri et al., 2021) or vehicle (30% β-cyclodextrin) was delivered (1.75 nmol) via an i.c.v. injection (2 μl) at the time of lorazepam administration.

2.5 | Plasma and brain concentration of AFC-5128

To ensure sufficiently high brain levels of the P2X7 receptor antagonist AFC-5128, mice were treated i.p. with 50 mg·kg⁻¹ AFC-5128, as before (Fischer et al., 2016). Plasma was prepared from blood collected into tubes containing 15 μl of 0.5-M EDTA (pH 7.4) via puncture of the saphenous vein 30 min following i.p. injection of 50 mg·kg⁻¹ AFC-5128. Plasma was prepared by centrifuging the tubes at 1300 × *g*, for 10 min at 4°C. Blood (terminal bleed) and brains were collected 60 min following 50 mg·kg⁻¹ AFC-5128 i.p. injection. Blood was immediately frozen down and brains removed following perfusion with ice cold PBS and immediately put on dry ice. Blood, plasma and brain samples from mice treated with AFC-5128 were analysed at the Lead Discovery Center (Dortmund, Germany). Briefly, AFC-5128 was extracted from plasma and homogenized brain by protein precipitation using acetonitrile. Resulting filtrates were analysed by liquid chromatography tandem-mass spectrometry (LC-MS/MS) using a Prominence UFLC system (Shimadzu, Duisburg, Germany) coupled to a QTrap 5500 instrument (ABSciex, Darmstadt, Germany). The compound was separated on a Zorbax Eclipse Plus C18 column (Agilent Technologies, Santa Clara, CA, USA) with an acetonitrile/water gradient containing 0.1% formic acid as solvent. Plasma, blood and brain concentrations were calculated by means of a standard curve (Fischer et al., 2016) (Figure S1).

2.6 | RNA extraction and qPCR

RNA extraction was performed using the Trizol method, as described before (Alves et al., 2019). Quantity and quality of RNA were measured using a Nanodrop Spectrophotometer (Thermo Scientific, Rockford, IL, USA). Samples with a 260/280 ratio between 1.8 and 2.0 were considered acceptable; 500 ng of total RNA was used to produce complementary DNA (cDNA) by reverse transcription using SuperScript III reverse transcriptase enzyme (Invitrogen, Waltham, MA, USA) primed with 50 pmol of random hexamers (Sigma). Quantitative real-time polymerase chain reaction (qPCR) was performed using the QuantiTech SYBR Green kit (Qiagen Ltd, Hilden, Germany) and the LightCycler 1.5 (Roche Diagnostics, GmbH, Mannheim, Germany). Each reaction tube contained 2 μ l cDNA sample, 10 μ l SyBR green Quantitect Reagent (Qiagen Ltd, Hilden, Germany), 1.25 μ M primer pair (Sigma) and RNase free water (Invitrogen) to a final volume of 20 μ l. Using LightCycler 1.5 software, data were analysed and normalized to the expression of β -actin. The primers used (Sigma) were as follows: *p2rx7* forward: actggcaggtgtgtgtccata, reverse: ttgcaagatgtttctctgtg; *p2rx2* forward: atgggattcgaattgacgtt, reverse: gatggtgggaatgagactgaa; *p2rx4* forward: tatgtgtcccagctcagga, reverse: tcacagacgcttgaatgga; *slc6a1* forward: gctcactctggtttccctcct, reverse: caccaacacagaaccaagg; *gria2* forward: actgctctgagaccctgaac, reverse: gagtgtgtgtctgttctgt; *gria5* forward: agctgtcgtgggattacaa, reverse: tgctgttctctgtgcaaac; *cx3cr1* forward: acagccagacaagaggagac, reverse: ccggagtcagtgaatgcatg; *aldh1l1* forward: tccaggcctagtccacaaag, reverse: attgggcagaattcgcattc; and β -actin forward: gggtgtgatgtgggaa, reverse: ggttgcccttagggttcagg.

2.7 | Western blotting

Western blot analysis was performed as described previously (Alves et al., 2019). The immuno-related procedures used comply with the recommendations made by the *British Journal of Pharmacology*. Lysis buffer (100-mM NaCl, 50-mM NaF, 1% Tx-100, 5-mM EDTA pH 8.0, 20-mM HEPES pH 7.4) containing a cocktail of phosphatase and protease inhibitors was used to homogenize hippocampal brain tissue and to extract proteins, which was quantified using a Tecan plate reader at 560 nm. Protein samples (30 μ g) were loaded onto an acrylamide gel and separated by SDS-PAGE. Following electrophoresis, proteins were transferred to a nitrocellulose membrane (GE Health Care, Chicago, IL, USA) and immunoblotted with P2X7 receptor extracellular primary antibody (1:400, prepared in 5% milk-Tris-buffered saline-Tween. TBST; anti-rabbit IgG; Alomone Labs, Jerusalem, Israel; Cat #: APR-008; RRID: AB_2040065) or Iba-1 (1:400 prepared in 5% milk-TBST; anti-rabbit; WAKO chemicals GMBH, Neuss, Germany; Cat #: 019-19741; RRID: AB_839504). Membranes were incubated with secondary antibody horseradish peroxidase-conjugated goat anti-rabbit (1:5000, prepared in 5% milk-TBST; rabbit-IgG; HRP; Millipore, Cork, Ireland; Cat #: AP132P; RRID: AB_90264). Protein bands were visualized using Fujifilm LAS-4000 system with chemiluminescence (Immobilon western HRP substrate, Merck Millipore, Cork,

Ireland) followed by analysis using Alpha-EaseFC4.0 software. Protein quantity was normalized to the loading control β -Actin (1:1000 prepared in 5% milk-TBST; anti-mouse; Sigma-Aldrich; Cat# A5316; re-used three to four times; RRID: AB_476743). Dilutions of the primary antibodies were kept at -20°C and re-used up to four times.

2.8 | Cytokine measurement in brain tissue

Levels of IL-1 β in the hippocampus were measured using the DuoSet ELISA kits from R&D Systems (Abingdon, UK) following the manufacturer's instructions (mouse IL-1 β /IL-1F2, Cat #: DY401-05). In a 96-well ELISA plate, the detection antibody was incubated overnight at room temperature. Then, 100 μ l of the samples (50 ng) and standard curve (IL-1 β : from 15.6–1000 $\text{pg}\cdot\text{ml}^{-1}$) were added to the wells and incubated for 2 h at room temperature, followed by incubation with 100 μ l of streptavidin-HRP complex. A colour reaction, caused by the addition of a substrate solution (100 μ l) and terminated via stopping solution (50 μ l), was quantified at 450 and 570 nm using a microplate reader. The cytokine concentration was obtained following the manufacturer's recommendations; 570 nm values were subtracted from the 450 nm values. The log₁₀ of the standard curve values were plotted, and a line of best fit was generated. The amount of cytokines was extrapolated using standard curve and average of calculated triplicate samples. Cytokine concentration was then expressed per mg of total protein in tissue.

2.9 | Fluoro-Jade B

Status epilepticus-induced neurodegeneration was analysed as before using Fluoro-Jade B (FJB) staining (Alves et al., 2019). Seventy-two hours post-status epilepticus, mice were transcardially perfused with 15 ml of PBS and brains were removed and flash frozen in 2-methylbutane (Sigma-Aldrich). Coronal tissue sections (12 μ m thick) at the medial level of the hippocampus (Bregma AP = -1.94 mm) were cut directly onto a glass slide using a CM1900 cryostat (Leica, Wetzlar, Germany) and stored at -80°C . Tissue was fixed in 4% paraformaldehyde (PFA), rehydrated in ethanol, and then transferred to a 0.006% potassium permanganate solution followed by incubation with 0.001% FJB (Chemicon Europe Ltd, Chandlers Ford, UK). DPX mounting solution was used to mount the sections. Using an epifluorescence microscope, FJB-positive cells including all hippocampal subfields (dentate gyrus [DG], CA1 and CA3) were counted, without knowledge of the treatment, under a 40x lens in two adjacent sections and the average determined for each animal.

2.10 | Histopathology

Sections from the same brains analysed for neurodegeneration using FJB were fixed in 4% PFA which was followed by permeabilization with 3% Triton and blocking with 5% goat serum. Sections were then

incubated overnight with the specific cell type markers: GFAP (1/400 prepared in 5% goat serum; rabbit-IgG; Sigma-Aldrich; Cat #: G9269; RRID:AB_477035) or Iba-1 (1:400 prepared in 5% goat serum; anti-rabbit; WAKO chemicals GMBH, Neuss, Germany; Cat #: 019-19741). Dilution of the primary antibodies was kept at -20°C and re-used up to three times. After rinsing with PBS, slices were incubated with secondary antibodies conjugated to AlexaFluor 568 (Cat #: A-11011; RRID:AB_143157) or 488 (Cat #: A11008; RRID:AB_2532697) (1/400 prepared in 5% goat serum; anti-rabbit-IgG; BioSciences, Dublin, Ireland) for 2 h at room temperature, followed by DAPI incubation. Sections were mounted using FluorSave (Merck Millipore), and two images from each hippocampal subfield were obtained using a $40\times$ lens in the Nikon 2000s epifluorescence microscope. The number of cells was then counted, without knowledge of the treatment, and the results presented as the average count from two images.

2.11 | Immunofluorescence

Mice were transcardially perfused with PBS (5 ml) and 4% PFA (10 ml) and brains removed. Following an additional 24 h long post-fixation in 4% PFA at 4°C , brains were transferred to PBS and immersed into 4% agarose. Sagittal sections ($30\ \mu\text{m}$) were cut using the VT1000S vibratome (Leica Biosystems, Wetzlar, Germany) and sections stored at -20°C in glycol. Tissue sections were incubated with 0.1% Triton/PBS, 1 M glycine, and with 1% BSA-PBS. Sections were then incubated with primary antibodies overnight: GFP (1:400 prepared in 1% BSA-PBS; rabbit-IgG; Life Science, Dublin, Ireland; Cat #: A11122; RRID:AB_221569), Iba-1 (1:400 prepared in 1% BSA-PBS; goat-IgG; Abcam, Cambridge, UK; Cat #: ab5076; RRID:AB_2224402), GFAP (1:400 prepared in 1% BSA-PBS; mouse-IgG; Sigma Aldrich; Cat #: AB5804; RRID:AB_2109645), β -Tubulin III (1:500 prepared in 1% BSA-PBS; mouse-IgG2a, κ ; Biolegend, San Diego, CA, USA; Cat #: MMS-435P; RRID:AB_2313773) and Oligo-2 (1:400 prepared in 1% BSA-PBS; mouse; clone 211F1.1; Millipore, Cork, Ireland; Cat #: MABN50). Dilution of the primary antibodies was kept at -20°C and re-used up to three times. After washing in PBS, tissue was incubated with fluorescent secondary antibodies, AlexaFluor 568 (Cat #: A-11011) or 488 (Cat #: A11008) (1/400 prepared in 1% BSA-PBS; anti-rabbit-IgG; BioSciences), followed by a short incubation with DAPI (1:500; Sigma-Aldrich). *FluorSave*[™] (Millipore, Dublin, Ireland) was used to mount the tissue. Confocal images were taken with a Zeiss 710 LSM NLO confocal microscope equipped with four laser lines (405, 488, 561 and 653 nm) using a $40\times$ immersion oil objective and ZEN 2010B SP1 software.

For double immunofluorescence (Figure 4a) with Iba-1 (1:200; mouse-IgG2a [κ light chain]; Synaptic Systems, Goettingen, Germany; Cat #: 234011; RRID:AB_2884925; re-used maximum three times) and P2X7 receptor (1:200; anti-mouse nanobody; Hamburg, Germany) stored tissue sections were washed with PBS and blocked with 0.05% saponin/3% BSA/15-mM NH_4Cl /PBS (blocking buffer) for 20 min. Primary antibodies were incubated overnight at 4°C in blocking buffer without saponin. After three washes with PBS, sections were

incubated for 2 h at room temperature with secondary antibodies, AlexaFluor-488 and AlexaFluor-647 (1:400; Life Technologies, Eugene, Oregon, USA), washed $3\times$ with PBS, shortly stained with DAPI ($1\ \text{mg}\cdot\text{L}^{-1}$, Carl Roth, Karlsruhe, Germany), washed with water and mounted (PermaFluor, Thermo Fisher, Dreieich, Germany) for confocal microscopy on a Zeiss LSM880 equipped with four laser lines (405, 488, 561 and 633 nm) using a $40\times$ immersion oil objective and ZEN 2.3 SP1 FP1 (black) software. Tissue thickness spanning Z-stacks were acquired in three arbitrary fields of view in the respective areas of the hippocampus and combined to maximum intensity projections using ZEN (blue edition) software.

2.12 | Three-dimensional morphological analysis of microglia

To analyse morphological changes of microglia, we carried out immunofluorescence staining, as described in the previous section. Microglia cells were identified via Iba-1 (1:400; anti-goat; Abcam; Cat #: ab5076; RRID:AB_2224402). The optimal number of slices was calculated using a Z Step Size calculator developed by the Cellular Imaging, Advanced Light Microscopy, Flow Cytometry and Electron Microscopy Centre, Amsterdam. Z-stacks of 100 slices (20- to $25\text{-}\mu\text{m}$ thickness, $0.1\text{-}\mu\text{m}$ interval) were taken with a Zeiss 710 LSM NLO confocal microscope using a $40\times$ immersion oil objective and ZEN 2010B SP1 software. Two Z-stacks were taken from each hippocampal subfield (i.e., CA1, CA3 and DG), amounting to six images per slice, $N = 3$ per group (naïve) and $N = 4$ per group (SE), totalling 42 stacks. Images were reconstructed with ImageJ to determine an average greyscale threshold value. Images were subsequently rendered in 3D using FluoRender Version 2.25.0. Three cells from each subfield were selected at random by a reviewer, blind to groups. Cells were isolated, with background noise removed as much as possible using the “diffusion paintbrush” option. Once removed, volumetric analysis was performed, using a minimum greyscale threshold value obtained from FIJI so as to only perform analysis on “real” signal, produced by antibody binding. Cell process length was then measured on the same software, using the multipoint measurement tool, beginning from the centre of the soma (located using DAPI) to the most extreme points of the cell process. Only primary processes were analysed, which means processes that extended directly from the soma, as opposed to secondary or tertiary processes branching of the primary cell process. Average process length was calculated as the mean length of all primary processes extending from the cell body of each individual cell.

2.13 | Ex vivo electrophysiology

Status epilepticus was induced in WT and P2X7R-OE mice, as described above (Section 2.2) and allowed to continue for 40 min. After this time, mice were killed by cervical dislocation for ex vivo brain slice preparation (mice were not treated with lorazepam and slices recorded without knowledge of genotype). Brains were quickly

dissected and submerged in oxygenated ice-cold sucrose artificial cerebrospinal fluid (ACSF; composition: in mM: 205 sucrose, 10 glucose, 26 NaHCO₃, 1.2 NaH₂PO₄·H₂O, 2.5 KCl, 5 MgCl₂, 0.1 CaCl₂); 400- μ m horizontal slices were prepared using a vibratome (Campden 7000 smz II, Campden Instruments, Loughborough, UK), with bath temperature held at \sim 1°C. Only slices from the hemisphere ipsilateral to KA injection were retained and stored at room temperature in a submerged-style holding chamber, filled with oxygenated ACSF (in mM: 125 NaCl, 10 glucose, 26 NaHCO₃, 1.25 NaH₂PO₄·H₂O, 3 KCl, 2 CaCl₂, 1 MgCl₂). For recording, slices were transferred to a membrane chamber which was perfused with oxygenated ACSF, heated to 34°C, at a rate of 16 ml·min⁻¹ (Morris et al., 2016). Slices were equilibrated to these conditions for 1 h prior to recording. A stimulating electrode (SS3CEA4-200, MicroProbes, MD, USA) was placed into the Schaffer collateral pathway, and 10 ms duration current pulses of varying amplitude were delivered using a DS3 isolated current stimulator (Digitimer, Welwyn Garden City, UK). Extracellular borosilicate glass recording electrodes (\sim 3 M Ω) were filled with ACSF and placed in strata radiatum (SR) and pyramidale (SP) in hippocampal CA1. Signal was acquired using a MultiClamp 700B amplifier (Molecular Devices, San Jose, CA, USA), Power 1401 digitiser (Cambridge Electronic Design, Cambridge, UK) and Signal software (v6, CED). Signals were digitized at 25 kHz and low pass filtered at 10 kHz. Data were analysed using Signal v6. Population spike was measured as the maximum trough amplitude recorded from CA1 SP and population synaptic potential as the slope of the response recorded in CA1 SR.

2.14 | Data, experimental design and statistical analysis

All experiments were carried out using male mice between 8 and 12 weeks of age, except in experiments corresponding to Figure 1, Figure 2, and Figure 3 which were carried out using both male and female P2X7R-OE mice, with the corresponding littermates. This manuscript complies with the recommendations of the *British Journal of Pharmacology* on experimental design and analysis. All experiments were designed to generate groups of equal size, using randomization and blinded analysis. To reduce unwanted sources of variation in our EEG analysis, the data were normalized to baseline or control groups, unless indicated otherwise. Group size is the number of independent values, and statistical analysis was done using these independent values, except for data presented in Figure 4b and Figure 5b,c where group size refers to individual cells/slice preparations analysed. Outliers were included in data analysis and presentation. In multigroup studies with parametric variables, post hoc tests were conducted only if *F* in ANOVA (or equivalent) achieved the chosen necessary level of statistical significance and there was no significant variance in homogeneity. Statistical information for experiments can be found in the Figure Legends, including control groups, group size and statistical test used. Statistical analysis of data was carried out using GraphPad Prism 5 and STATVIEW software (SAS Institute, Cary, NC, U.S.A).

Data are presented as means \pm SEM. One-way ANOVA parametric statistics with post hoc Fisher's protected least significant difference test was used to determine statistical differences between three or more groups. Unpaired Student's *t* test was used for two-group comparisons. Two-way ANOVA was used for repeated measures between groups where a series of measurements have been taken from the same mouse at different time-points. Statistical analysis was undertaken only for studies where each group size was at least *N* = 5. Other data where group sizes were below *N* = 5, are indicated as preliminary data. Significance was accepted at **P* < 0.05.

2.15 | Materials

2-Hydroxypropyl- β -cyclodextrin, carbamazepine, *N,N*-dimethylacetamide, kainic acid, LPS, midazolam, minocycline, and phenytoin were supplied by Sigma-Aldrich. AFC-5128 was supplied by Affectis Pharmaceuticals AG (Dortmund, Germany); ITH15004 by Fundación Teófilo Hernando (Madrid, Spain), lorazepam by Wyeth (Taplow, UK) and MCC950 by InvivoGen (Toulouse, France).

2.16 | Nomenclature of targets and ligands

Key protein targets and ligands in this article are hyperlinked to corresponding entries in <http://www.guidetopharmacology.org>, and are permanently archived in the Concise Guide to PHARMACOLOGY 2021/22 (Alexander, Christopoulos, et al., 2021; Alexander, Fabbro, et al., 2021; Alexander, Mathie, et al., 2021).

3 | RESULTS

3.1 | Mice overexpressing P2X7 receptors show reduced responsiveness to lorazepam during status epilepticus

Expression of P2X7 receptors in the brain increases under several pathological conditions associated with the development of status epilepticus including stroke, TBI and infection (Di Virgilio et al., 2017; Franke et al., 2004; Liu et al., 2017). It is uncertain, however, whether elevated P2X7 receptor expression contributes to the development and persistence of seizures, to sensitivity to anti-seizure medication, or both. To address this question, we first studied status epilepticus in mice overexpressing P2X7 receptor C-terminally fused to the fluorescent protein EGFP (P2X7R-OE mice) (Kaczmarek-Hajek et al., 2018). Status epilepticus was triggered by intra-amygdala KA, as described (Figure 1a). All mice were treated with an anticonvulsant, typically lorazepam, after 40 min post-KA injection to model a clinically realistic scenario and reduce both mortality and morbidity.

As reported previously (Kaczmarek-Hajek et al., 2018), hippocampal expression of mRNA for P2X7 receptors in untreated P2X7R-OE mice was about seven-fold higher than that in WT mice

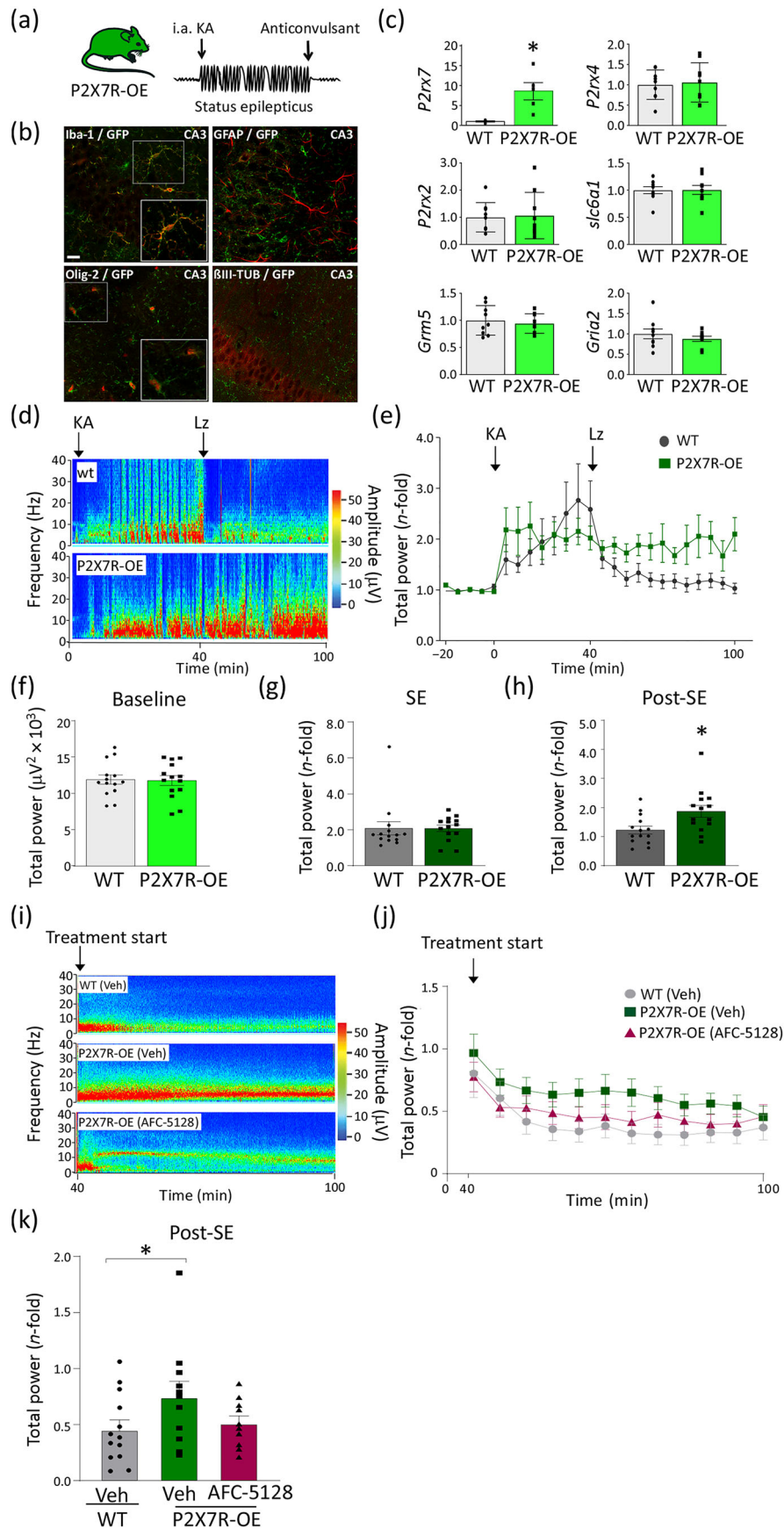


FIGURE 1 Legend on next page.

FIGURE 1 Mice overexpressing P2X7 receptors (P2X7R-OE) undergoing status epilepticus are resistant to the anticonvulsant lorazepam. (a) Status epilepticus (SE) was induced via an injection of KA into the basolateral nucleus of the ipsilateral amygdala (i.a. KA) in mice. First seizure bursts appear usually within minutes and gradually develop into status epilepticus. To reduce mortality and morbidity, the anticonvulsant lorazepam (Lz) was administered 40 min post-KA injection. (b) Photomicrographs (40 \times lens) showing co-localization of P2X7R-EGFP (green) with microglia marker Iba-1 (red) and oligodendrocyte marker Olig-2 (red) in the CA3 region of the hippocampus under naïve conditions. Co-localization of P2X7R-EGFP (green) with the astrocyte marker GFAP or with the neuronal marker β III-Tub (red) was not detected. Scale bar = 20 μ m. (c) Graph showing higher *P2rx7* mRNA levels in the hippocampus of naïve P2X7R-OE mice, compared with naïve wild-type (WT) mice. No difference was observed in hippocampal mRNA levels for *P2rx4*, *P2rx2*, *slc6a1*, *Gria2* and *Grm5* between naïve P2X7R-OE and naïve WT mice ($N = 9$ per group). Data were normalized to β -actin and are shown as individual values with means \pm SEM. * $P < 0.05$, significantly different from WT; unpaired Student's *t* test. (d) Representative EEG recordings presented as heat maps of frequency and amplitude data of WT and P2X7R-OE mice from the time of KA injection until 60 min post-lorazepam treatment. (e) Graph showing EEG total power during a 100-min recording period ($N = 14$ per group). (f) No difference was observed at baseline (20 min) or (g) during 40 min of status epilepticus in EEG total power between P2X7R-OE and WT mice ($N = 14$ per group). (h) Graph showing a significant increase in EEG total power in P2X7R-OE mice, compared with WT mice, post-status epilepticus (post-lorazepam administration). Data are shown as individual values with means \pm SEM; $N = 14$ per group. * $P < 0.05$, significantly different from WT; unpaired Student's *t* test. (i) Representative EEG recordings presented as heat maps of frequency and amplitude data of WT and P2X7R-OE mice treated with P2X7R antagonist AFC-5128 or vehicle at the time of lorazepam. (j) Graph showing EEG total power of WT and P2X7R-OE mice subjected to intra-amygdala KA treated with vehicle or P2X7R antagonist AFC5128 from the time of lorazepam/P2X7R antagonist administration (40 min post-KA) until 100 min post-KA treatment. (k) Graph showing a significant increase in EEG total power in P2X7R-OE-vehicle mice, compared with vehicle-treated WT mice post-status epilepticus. Total seizure power post-status epilepticus was normalized to severity of status epilepticus (time of KA injection until treatment with lorazepam) for each mouse. Data are shown as individual values with means \pm SEM; $N = 13$ (WT, Veh), 11 (P2X7R-OE, Veh) and 10 (P2X7R-OE, AFC-5128). * $P < 0.05$, significantly different as indicated; one-way ANOVA with post hoc Fisher's test

and restricted mainly to microglia and oligodendrocytes (Figure 1b, c). Hippocampal expression of **P2X4** and **P2X2** receptors was unaltered in P2X7R-OE mice, indicating that transgenic overexpression of P2X7 receptors did not affect expression of other P2X receptors (Figure 1c). Moreover, P2X7R-OE mice showed normal hippocampal expression of genes involved in epilepsy-associated neurotransmitter systems including the sodium- and chloride-dependent GABA transporter 1 (*Slc6a1*), glutamate metabotropic receptor 5 (*Grm5*) and glutamate ionotropic receptor AMPA type subunit 2 (*Gria2*) (Figure 1c).

Next, to test whether P2X7 receptor overexpression affects status epilepticus or responses to anticonvulsants, EEGs of P2X7R-OE and WT mice were compared upon KA injection. This included a 10-min baseline recording before KA injection, 40 min between intra-amygdala KA and lorazepam (status epilepticus) administration, and an additional 60 min following lorazepam treatment (post-status epilepticus). EEG baseline recordings, measured as total power, were similar between WT and P2X7R-OE mice (Figure 1d–f). This suggests that WT and P2X7R-OE mice are equally sensitive to intra-amygdala KA. Likewise, no difference in seizure severity measured as EEG total power and behaviour changes was observed between genotypes from the time of intra-amygdala KA until treatment with lorazepam (Figures 1d,e,g and S2). However, whereas lorazepam produced a sustained reduction in status epilepticus severity in WT mice (measured as EEG total power), lorazepam was significantly less effective in reducing seizures in P2X7R-OE mice (Figure 1d,e,h). This suggests that overexpression of P2X7 receptors and signalling may interfere with the normal anticonvulsant effect on SE. To test this hypothesis, P2X7R-OE mice were treated with the P2X7 receptor antagonist

AFC-5128 and lorazepam together. As before, untreated P2X7R-OE mice showed a reduced response to lorazepam when compared with WT mice (Figure 1i–k). In contrast, no difference in seizure severity, post-status epilepticus, was observed between WT and AFC-5128-treated P2X7R-OE mice (Figure 1k).

We next analysed neuronal damage 72 h post- status epilepticus in the brains of these mice. Neurodegeneration, as assessed by the number of FjB-positive cells, was similar between groups (Figure 2a). However, P2X7R-OE mice displayed more Iba-1 positive cells in all hippocampal subfields and more GFAP-positive cells in CA1, compared with WT mice (Figure 2b,c). Taken together, these findings indicate that P2X7 receptor overexpression reduced responsiveness to lorazepam during status epilepticus and exacerbated gliosis, without affecting neurodegeneration.

3.2 | P2X7 receptor overexpression causes broad resistance to anticonvulsants during status epilepticus

To test whether P2X7 receptor overexpression contributes to broad drug-unresponsiveness in status epilepticus, we tested three additional commonly used ASDs for status epilepticus in our model. These were the positive allosteric GABA receptor modulator midazolam and the anticonvulsive drugs, phenytoin and carbamazepine. For the latter, the exact mechanism of action is not known but appears to involve sodium channel blocking.

As before, no differences could be observed in seizure severity between WT and P2X7R-OE mice during the time from intra-amygdala KA until the administration of anticonvulsants 40 min later (Figure 3a–c). In contrast and as observed for lorazepam, all

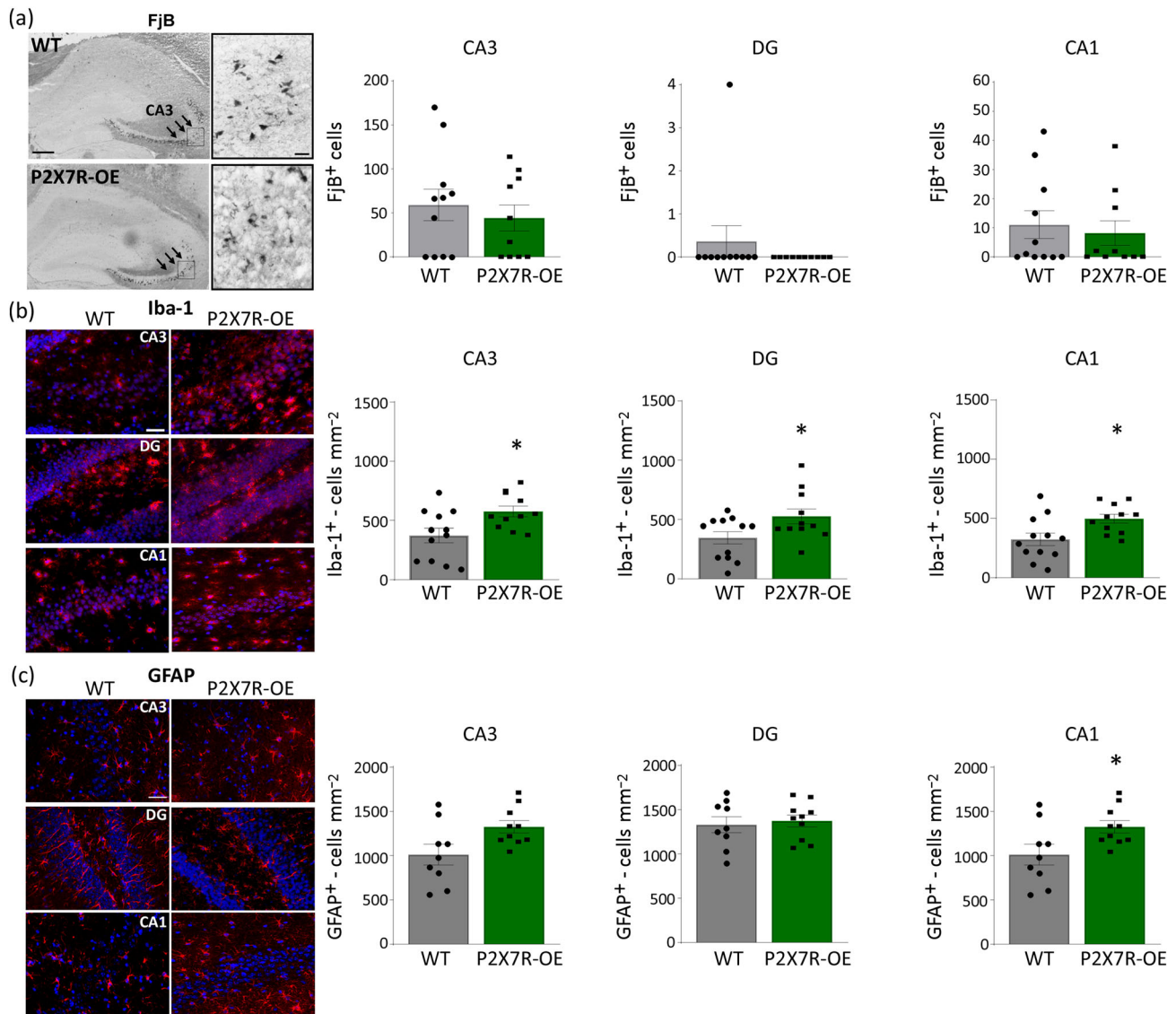


FIGURE 2 Status epilepticus-induced brain pathology in P2X7R overexpressing (P2X7R-OE) mice. (a) Representative image (5× lens) and bar graphs showing no difference in cell death between P2X7R-OE mice and WT mice in the hippocampal subfields CA3, CA1 and dentate gyrus (DG) 72 h post-intra-amygdala KA-induced status epilepticus as shown by FJB-positive cells (arrows and insert). Scale bar 500 μm (left panel) and 50 μm (right panel) (N = 11 WT and 10 P2X7R-OE). (b) Immunofluorescence and graphs showing a significant increase in Iba-1 positive cells 72 h post-SE, in the different subfields of the hippocampus (CA3, CA1 and DG) in P2X7R-OE mice, compared with WT mice. Data are shown as individual values with means ± SEM; N = 12 WT and 11 P2X7R-OE. *P < 0.05, significantly different from WT; unpaired Student's *t* test. (c) Representative images and graph showing an increase in GFAP-positive cells in the CA1 subfield of the hippocampus in P2X7R-OE mice, compared with WT mice. No differences between genotypes of GFAP-positive cells were found in CA3 and DG. Data are shown as individual values with means ± SEM; N = 9 WT and 10 P2X7R-OE. *P < 0.05, significantly different from WT; unpaired Student's *t* test. Scale bar = 50 μm

tested anticonvulsants were ineffective at curtailing status epilepticus in P2X7-OE mice. While WT mice responded to each anticonvulsant with a gradual suppression of seizure severity, seizures continued in P2X7R-OE mice. Again, analysis of brain sections from these mice showed that, while overall neurodegeneration was similar between genotypes 72 h post-status epilepticus (Figure 3a–c), microgliosis was increased in the hippocampus of P2X7R-OE mice (Figure 3a–c).

3.3 | P2X7 receptor overexpression-induced unresponsiveness to anticonvulsants is a consequence of increased inflammation

We next aimed to understand how P2X7 receptors contribute to the development of drug-resistant status epilepticus. P2X7 receptors are highly expressed on microglia during physiological conditions and post-status epilepticus, and their involvement in microglia activation

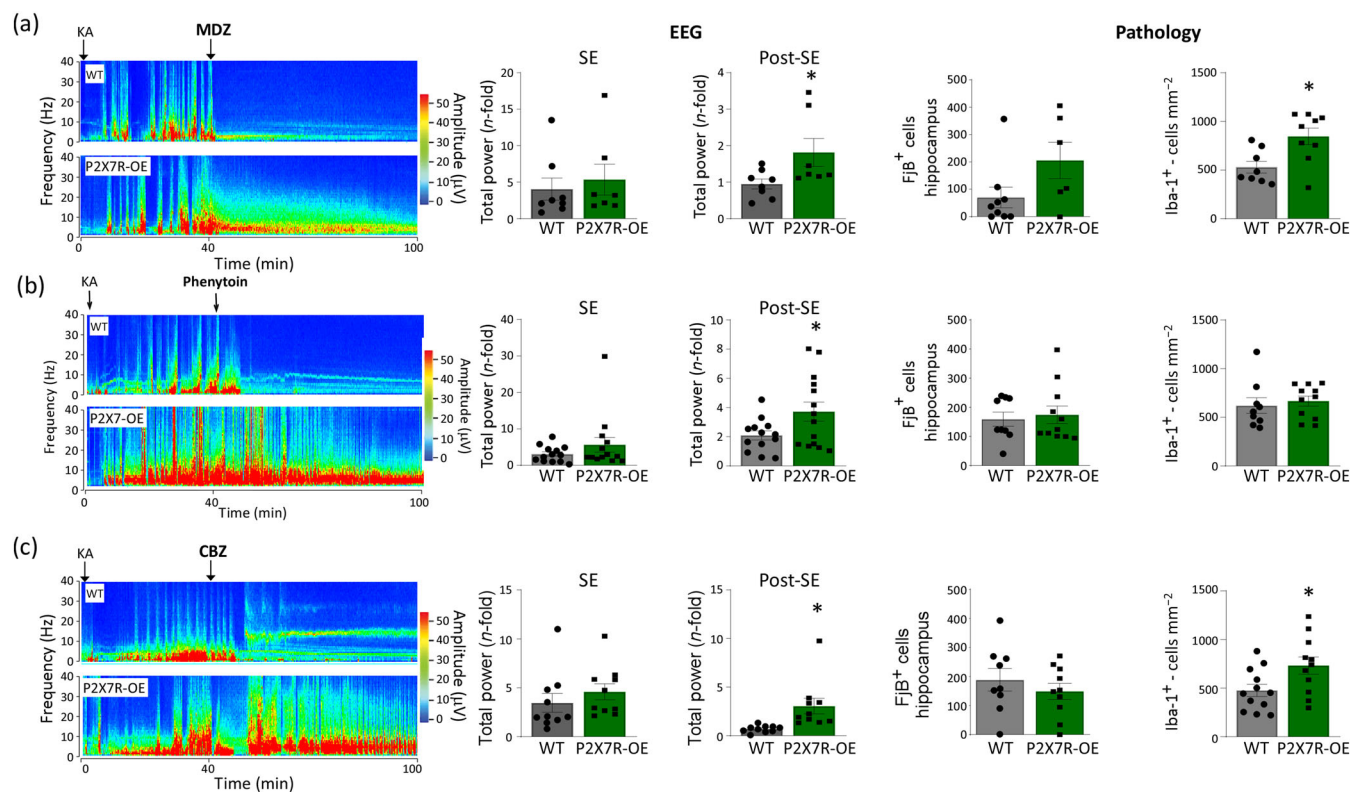


FIGURE 3 P2X7R overexpressing (P2X7R-OE) mice are resistant to anticonvulsant drugs. (a) Representative EEG recordings presented as heat maps of frequency and amplitude data of WT and P2X7R-OE mice. No difference was observed in the EEG total power between WT and P2X7R-OE mice during status epilepticus. EEG total power was, however, significantly higher in P2X7R-OE mice, compared with WT mice, post-status epilepticus, after i.p. midazolam (MDZ). Data are shown as individual values with means \pm SEM; $N = 8$ WT and 7 P2X7R-OE. Graph showing no difference in cell death in P2X7R-OE mice, compared with WT mice, in the hippocampus 72 h following KA-induced status epilepticus when treated with MDZ; $N = 9$ WT and 6 P2X7R-OE. P2X7R-OE mice show more Iba-1-positive cells compared to WT mice in the hippocampus, 72 h following KA-induced status epilepticus; $N = 8$ WT and 9 P2X7R-OE. Data are shown as individual values with means \pm SEM. $*P < 0.05$, significantly different from WT; unpaired Student's t test. (b) Representative EEG recordings presented as heat maps of frequency and amplitude data of WT and P2X7R-OE mice. While no difference in EEG total power was observed during SE, EEG total power was significantly higher in P2X7R-OE mice post-status epilepticus (after treatment with phenytoin); $N = 13$ WT and 14 P2X7R-OE. No difference in FjB- or Iba-1-positive cells between P2X7R-OE mice and WT mice 72 h post-status epilepticus; $N = 9$ WT and 11 P2X7R-OE mice. Data are shown as individual values with means \pm SEM. $*P < 0.05$, significantly different from WT; unpaired Student's t test. (c) Representative heat maps and graphs showing no difference in the total power between P2X7R-OE and WT mice during status epilepticus. EEG total power was significantly higher in P2X7R-OE mice compared with WT mice, post-status epilepticus, after i.p. carbamazepine (CBZ); $N = 10$ per group). No difference in the number of FjB-positive cells in the hippocampus between P2X7R-OE mice, compared with WT mice, 72 h post-status epilepticus; $N = 9$ WT and 10 P2X7R-OE. Significant increase in Iba-1-positive cells in P2X7R-OE mice in the hippocampus 72 h following status epilepticus; $N = 11$ WT and 12 P2X7R-OE. Data are shown as individual values with means \pm SEM. $*P < 0.05$, significantly different from WT; unpaired Student's t test

and proliferation has been described (Monif et al., 2009). Moreover, microglia are among the first cell types to respond to injury, and this is mediated via extracellular ATP (Davalos et al., 2005). We therefore hypothesized that the effects of P2X7 receptor overexpression during status epilepticus are mediated, at least in part, via its pro-inflammatory function in microglia and focused on this cell type.

Double-immunostaining of brain sections from WT mice collected 60 min post-intra-amygdala KA injection, a time-point when sensitivity to lorazepam is reduced in this model (Engel et al., 2012), showed a more intense staining of P2X7 receptors on Iba-1-positive microglia in the hippocampus including all three hippocampal subfields. Microglia analysed at the same time-point showed also an increased

immunoreactivity to Iba-1 and larger cell bodies, indicating a more activated state (Figures 4a and S3). These findings are consistent with status epilepticus driving an early up-regulation of P2X7 receptors in microglia that might influence their inflammatory state and suggest that P2X7 receptor-driven unresponsiveness to anticonvulsants is mediated, at least in part, via microglia-driven inflammation. To test this idea, WT and P2X7R-OE mice were pretreated with the broad-spectrum anti-inflammatory drug minocycline ($30 \text{ mg} \cdot \text{kg}^{-1}$) 24 and 4 h prior to inducing status epilepticus (Figure 4b). Confirming its selective effect on microglial inflammatory signalling, minocycline treatment reduced hippocampal transcription of the microglia marker fractalkine receptor *Cx3Cr1* without affecting transcript levels of the

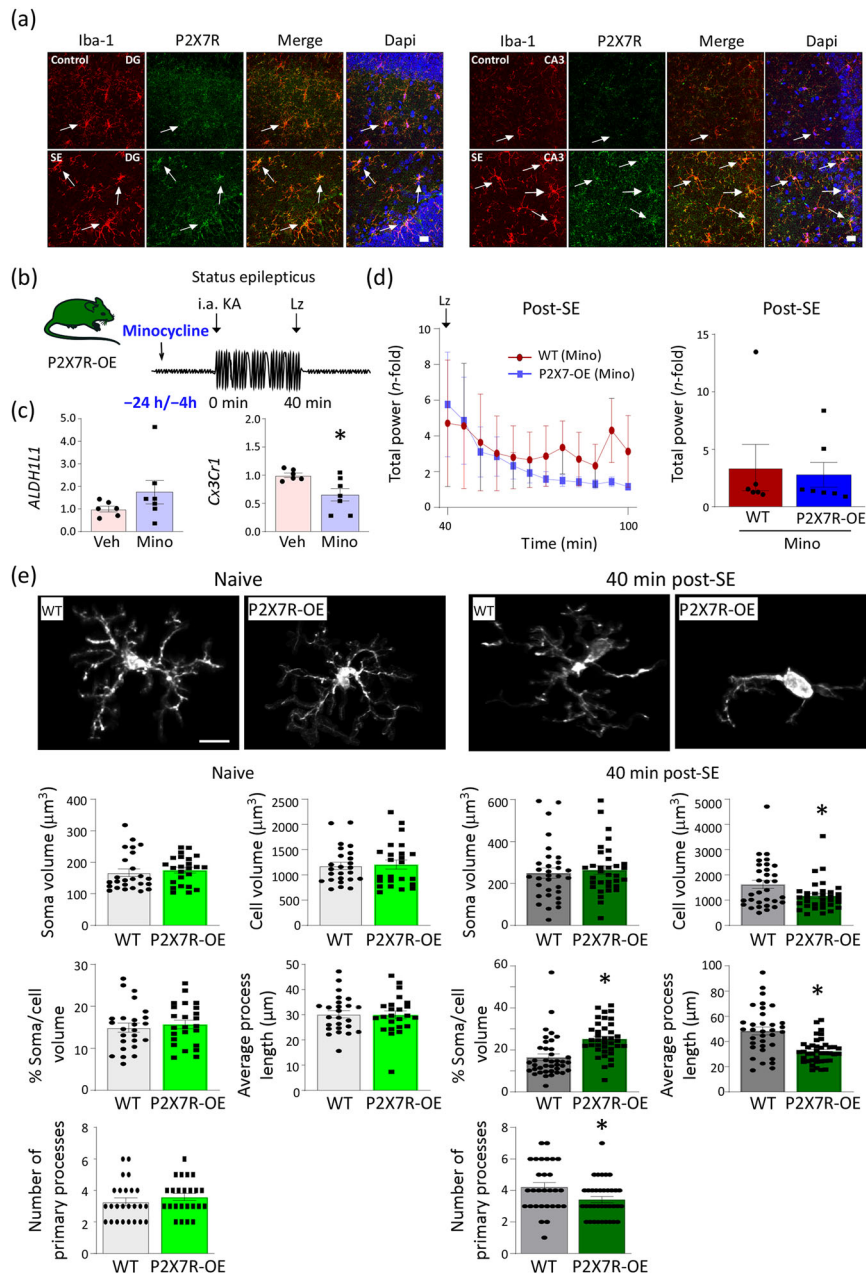


FIGURE 4 P2X7R diminishes responses to anticonvulsants during status epilepticus via driving inflammation. (a) Representative images showing co-localization of P2X7R (green) with Iba-1-positive microglia (red) in the hippocampal subfield DG and CA3 in C57/Bl6 WT mice under control conditions and 60 min post-intra-amygdala KA injection. Note, while P2X7R immunoreactivity is almost absent in control mice, P2X7R immunoreactivity increases strongly in Iba-1-positive microglia 60 min post-KA injection. Immunostaining was repeated in three individual mice per group obtaining similar results. Scale bar = 20 μm . (b) Experimental design using the broad-spectrum anti-inflammatory agent, minocycline (Mino). P2X7R-OE mice were treated with minocycline (30 $\text{mg}\cdot\text{kg}^{-1}$, i.p.) 4 and 24 h before intra-amygdala KA-induced status epilepticus. (c) Minocycline treatment leads to a reduction in hippocampal Cx3Cr1 mRNA levels. No difference was observed in hippocampal ALDH1L1 mRNA levels. Data are shown as individual values with means \pm SEM; $N = 6$ vehicle and 7 minocycline. * $P < 0.05$, significantly different from WT; unpaired Student's t test. (d) Graphs showing no difference in EEG total power between WT and P2X7R-OE mice treated with minocycline post-status epilepticus (post-SE; time between 40 min post-KA until 100 min post-KA). Data are shown as individual values with means \pm SEM; $N = 6$ vehicle and 7 minocycline. (e) Representative pictures of microglia in WT and P2X7R-OE mice during naïve conditions and 40 min post-intra-amygdala KA injection. Scale bar = 10 μm . In naïve conditions, no difference in soma volume, cell volume, ratio between somatic/cell volume, average processes length and number of processes per microglia was observed between P2X7R-OE and WT mice. However, 40 min post-status epilepticus, graphs showed a significant increase in the cell volume, the ratio of somatic to /cell volume, the average length of processes and the number of processes per microglia in P2X7R-OE mice, compared with WT mice. $N = 25$ cells from WT, naïve and 24 cells from P2X7R-OE, naïve; 28 cells from WT, status epilepticus and 37 cells from P2X7R-OE, status epilepticus. Cells were analysed in three mice per genotype under naïve conditions and four mice per genotype post-KA injection. Data are shown as individual values with means \pm SEM. * $P < 0.05$, significantly different from WT; unpaired Student's t test.

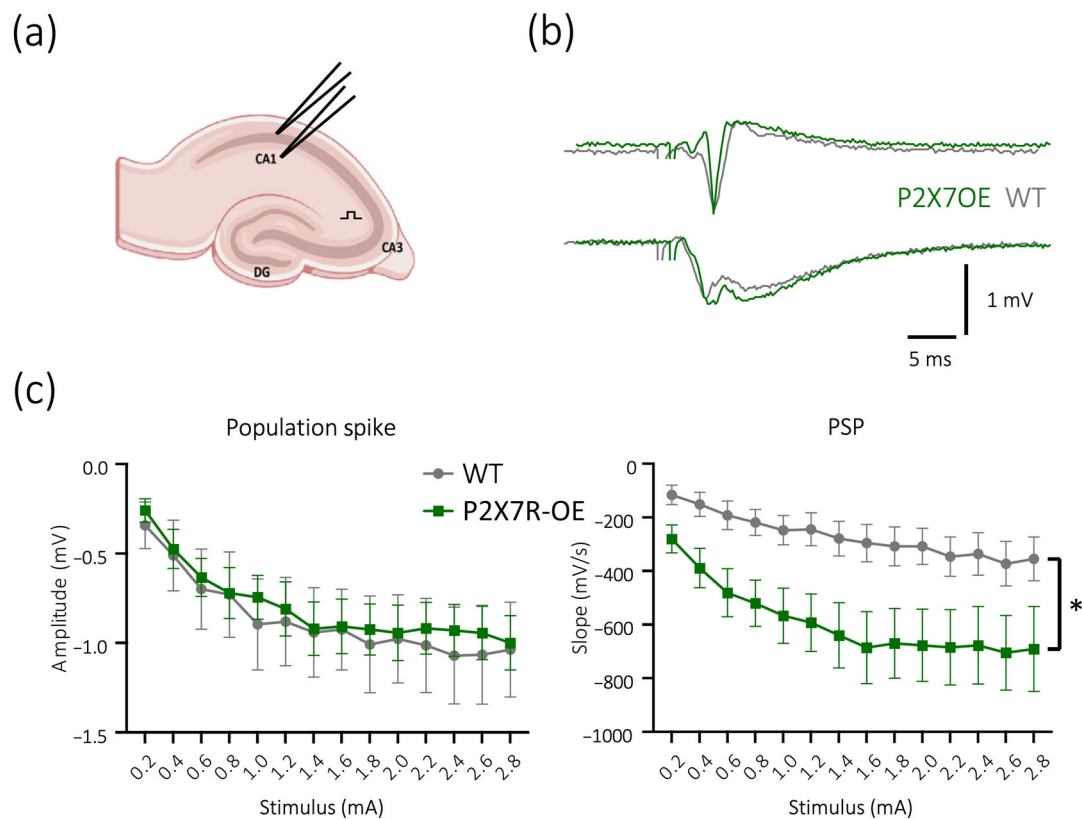


FIGURE 5 P2X7R-OE mice exhibit more network excitability in the hippocampus after status epilepticus (post-SE). (a) Diagram showing electrode placement. A stimulating electrode was placed in the Schaffer collateral pathway, and two recording electrodes placed in CA1 strata pyramidale (for population spike) and radiatum (for population postsynaptic potential). (b) Representative traces taken from P2X7R-OE and WT mice, after 40 min of status epilepticus. (c) Overall data (means \pm SEM) show that population spike amplitude was unchanged between P2X7R-OE and WT mice. Population synaptic potential (PSP) slope was significantly higher in P2X7R-OE mice after 40 min status epilepticus. All data are from $N = 4$ mice per genotype and two to three slices per mouse. * $P < 0.05$, significant effect of treatment; repeated measures two-way ANOVA

astrocyte marker *ALDH1L1*, as reported previously (Figure 4c) (Alves et al., 2019; Kobayashi et al., 2013). No difference in response to lorazepam treatment was seen between P2X7R-OE and WT mice, if mice were pretreated with minocycline (Figure 4d). This is consistent with the hypothesis that a reduced response to anticonvulsants in P2X7R-OE mice is partly mediated by increased inflammation. Notably, we found no gross differences in microglia morphology between WT and P2X7R-OE mice under naïve conditions with microglia from both genotypes showing similar volumes of both soma and whole cell bodies including all microglial processes, thus displaying the typical morphology of resting microglia (Figure 4e). In contrast, microglia from P2X7R-OE mice obtained 40 min post-KA injection showed a slightly smaller cell volume and significantly less primary processes than those from WT mice (Figure 4e), consistent with a more activated, amoeboid and pro-inflammatory phenotype.

Finally, to investigate whether there is an effect of P2X7 receptor overexpression on brain network activity during status epilepticus (40 min post-KA treatment), we analysed electrophysiological responses in hippocampal slices from WT and P2X7R-OE mice subjected to status epilepticus (Figure 5a). This revealed that slices from

P2X7R-OE mice displayed an increased population synaptic potential in hippocampal CA1, indicating greater synaptic activation within the hippocampal network, which may contribute to the diminished response to anticonvulsants observed in these animals (Figure 5b,c).

3.4 | P2X7 receptor overexpression effects during status epilepticus are independent of NLRP3 inflammasome activation

As overexpression of the P2X7 receptor impaired responses to anticonvulsants during status epilepticus, we reasoned that loss of these receptors may improve their efficiency. As shown for P2X7R-OE mice, *P2X7^{-/-}* mice showed a normal expression of genes involved in neurotransmission including *Slc6a1*, *GRM5* and *Gria2* (Figure 6a). As reported previously, using the same *P2X7^{-/-}* strain (Conte et al., 2020), *P2X7^{-/-}* mice and WT mice showed similar seizure severity during status epilepticus (Figure 6b,c). However, in line with the P2X7 receptor contributing to anticonvulsant unresponsiveness during status epilepticus, *P2X7^{-/-}* mice showed a better response to

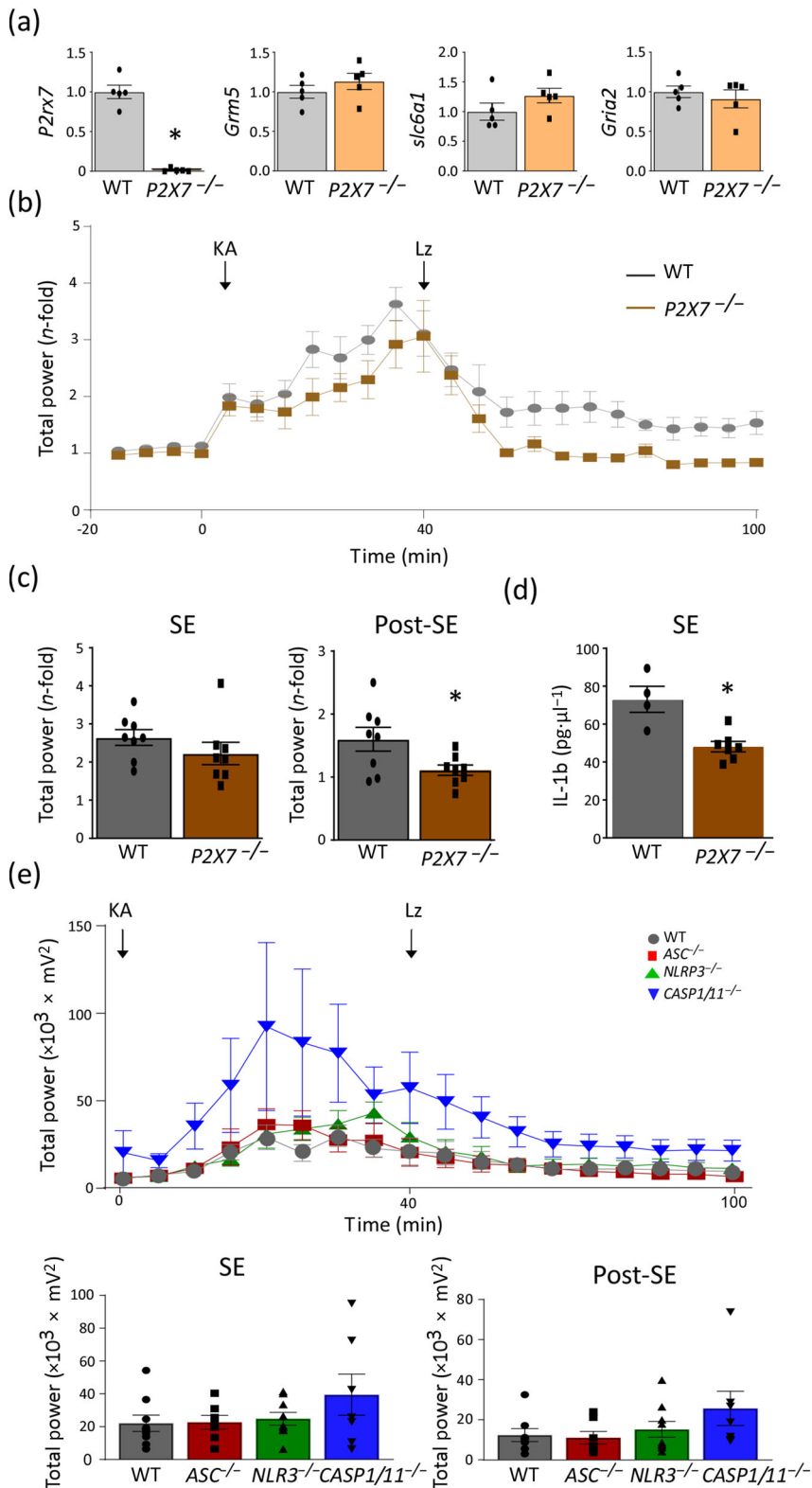


FIGURE 6 P2X7R effects during status epilepticus are independent of the P2X7R-NLRP3 axis. (a) Graph showing absence of *P2rx7* transcripts in the hippocampus of *P2X7* KO mice (*P2X7*^{-/-}), compared with WT mice, in naïve conditions. Data are shown as individual values with means ± SEM; N = 5 per group. **P* < 0.05, significantly different from WT; unpaired Student's *t* test. No difference in hippocampal mRNA levels of *Grm5*, *slc6a1* and *Gria2* in *P2X7*^{-/-} mice, compared with WT mice, under naïve conditions (N = 5 per group). (b, c) No difference in EEG total power between WT and *P2X7*^{-/-} mice from the time of intra-amygdala KA until lorazepam administration 40 min later. Reduced EEG total power in *P2X7*^{-/-} mice compared with WT mice, during a 60-min recording period post-status epilepticus (post-SE). Data are shown as individual values with means ± SEM; N = 8 per group. **P* < 0.05, significantly different from WT; unpaired Student's *t* test. (d) Graph showing a reduction in the level of the cytokine IL-1β in *P2X7*^{-/-} mice 40 min following intra-amygdala KA treatment. Data are shown as individual values with means ± SEM; N = 4 (WT) and 7 (*P2X7*^{-/-}). **P* < 0.05, significantly different from WT; unpaired Student's *t* test. (e) No difference was observed in the EEG total power during and after status epilepticus, between WT and *ASC*^{-/-}, *NLRP3*^{-/-} and *CASP1*^{-/-} mice. N = 9 (WT), 7 (*ASC*^{-/-}), 9 (*NLRP3*^{-/-}) and 7 (*CASP1*^{-/-})

lorazepam when compared with WT mice (Figure 6b,c). ELISA assays using hippocampal tissue extracted 40 min post-intra-amygdala KA showed reduced IL-1β levels in *P2X7*^{-/-} mice, when compared with WT mice (Figure 6d), suggesting altered inflammatory pathways in *P2X7*^{-/-} mice.

The P2X7 receptor has been described as one of the main activators of the NLRP3 inflammasome leading to the release of IL-1β (Pelegrin, 2021). If effects of P2X7 receptors on responsiveness to anticonvulsants during status epilepticus were mediated via the P2X7 receptor-NLRP3 axis, then responses of mice deficient in components

of the NLRP3 signalling pathway should mimic the improved response of $P2X7^{-/-}$ mice during status epilepticus. To test this hypothesis, caspase-1/11, NLRP3 or the inflammasome adaptor protein apoptosis-associated speck-like protein containing a CARD (ASC) KO mice were subjected to intra-amygdala KA and seizure severity, compared with WT mice. Unexpectedly, no significant differences were observed between WT mice and the different KO strains either during status epilepticus or post-lorazepam administration (Figure 6e), suggesting that resistance to anticonvulsants is NLRP3-independent. Of note, although not statistically different, $Casp\ 1/11^{-/-}$ mice showed consistently increased seizure severity when compared with WT mice. Moreover, no significant difference in hippocampal neurodegeneration between genotypes could be observed 72 h post-status epilepticus (Figure S4).

Taken together, our results suggest that the effects of the P2X7 receptor on anti-convulsant drug responses during status epilepticus involve microglia activation but are independent of NLRP3 inflammasome activation and that NLRP3 inflammasome inhibition has no effect on seizure severity or neuropathology in the intra-amygdala KA mouse model.

3.5 | P2X7 receptor antagonists improve responses to anticonvulsants during status epilepticus in mice pretreated with LPS

We next sought to explore whether P2X7 receptor antagonism could be effective in a more clinically-relevant model of elevated inflammatory tone at the time of status epilepticus, compared to our genetic model. To induce inflammation, mice were pretreated i.p. with the bacterial component LPS (Beutler & Poltorak, 2000), prior to intra-amygdala KA (Figure 7a). Preliminary data shows that treatment with LPS led to increases in Iba-1 and P2X7 receptor protein expression in the hippocampus, 72 h post-LPS treatment (Figure 7b). Next, we sought to establish whether LPS-treated mice, similar to P2X7R-OE mice, were also less responsive to anticonvulsants during status epilepticus and, if so, whether deletion or blocking of P2X7 receptors could reverse LPS-induced drug-unresponsiveness. EEG analysis revealed that, whereas vehicle-treated WT mice showed seizure severity during status epilepticus, similar to that in LPS-treated WT mice, they responded significantly better to anticonvulsant treatment than LPS-pretreated mice (Figure 7c). Further supporting a P2X7 receptor-mediated drug unresponsiveness, LPS-pretreated $P2X7^{-/-}$ mice responded ~50% better to the anticonvulsant lorazepam administered 40 min post-intra-amygdala KA than LPS-pretreated WT mice (Figure 7d). EEG-recorded seizures were similar before lorazepam administration (Figure 7d). These results with LPS-pretreated P2X7 receptor-deficient mice could be replicated by administration of two P2X7 receptor antagonists, AFC-5128 or ITH15004, to LPS-pretreated WT mice: Mice treated with both P2X7R antagonists at the time of lorazepam treatment responded better (~40% reduction in seizures) to lorazepam than vehicle-injected LPS pretreated mice

(Figure 7e,f). Again, further supporting the conclusion that P2X7R-mediated effects on responsiveness to anticonvulsants are independent of NLRP3 inflammasome activation, WT mice pretreated i.p. with LPS and injected with the NLRP3 inflammasome inhibitor MCC950 40 min post-KA, experienced even more severe seizures (~2.5-fold increase), following the administration of lorazepam (Figure S5).

In summary, we conclude that P2X7 receptor expression was increased under inflammatory conditions in the brain, leading to a lower response to anticonvulsants during status epilepticus. Inhibition of P2X7 receptors, therefore, represents a promising novel treatment strategy for status epilepticus where underlying neuroinflammation is one of the pathological hallmarks.

4 | DISCUSSION

By using genetic and pharmacological approaches, we have been able to show that P2X7 receptors contribute to unresponsiveness to anticonvulsants during status epilepticus. We further show that these effects are most likely mediated via a P2X7 receptor-activated pro-inflammatory mechanism. Genetic deletion and pharmacological inhibition of P2X7 receptors restored normal responses to ASDs during status epilepticus, thus demonstrating the therapeutic potential of P2X7 receptor-targeting therapies as novel adjunctive treatment for RSE.

Several neurotransmitter systems have been implicated in the generation of RSE, in particular GABAergic and glutamatergic neurotransmission (Betjemann & Lowenstein, 2015). Here, we show that the purinergic ATP-gated P2X7 receptor contributes to unresponsiveness to anticonvulsants during status epilepticus, thereby proposing an additional neurotransmitter system that contributes to RSE. Our data showed an early increase in P2X7 receptor expression during status epilepticus in WT mice, in line with the early occurrence of drug resistance. A functional role of ATP-gated receptors during status epilepticus was further demonstrated by data showing that the administration of ATP and the ATP analogue **2',3'-O-(4-benzoyl-benzoyl)ATP (BzATP)** into the brain increases seizure severity during status epilepticus (Engel et al., 2012; Sebastian-Serrano et al., 2016). Moreover, P2X7 receptors appear to interfere with drug responses at later time-points, when refractoriness to anticonvulsants becomes evident (Engel et al., 2012). P2X7 receptors are activated by high extracellular concentrations of ATP ($EC_{50} \geq 100 \mu\text{M}$) (Surprenant et al., 1996), most likely reached under ongoing pathological conditions, such as prolonged seizures and sustained inflammation (Vezzani et al., 2011). Also, its high activation threshold (0.3- to 0.5-mM ATP) decreases during inflammatory conditions (0.05- to 0.1-mM ATP) (Di Virgilio et al., 2017). Several studies have shown only moderate or no anticonvulsant effects of P2X7 receptor antagonism during acute seizures such as in the maximal electroshock, the pentylenetetrazol and the 6 Hz psychomotor test (Fischer et al., 2016; Nieoczym et al., 2017). This is in line with the need for an ongoing

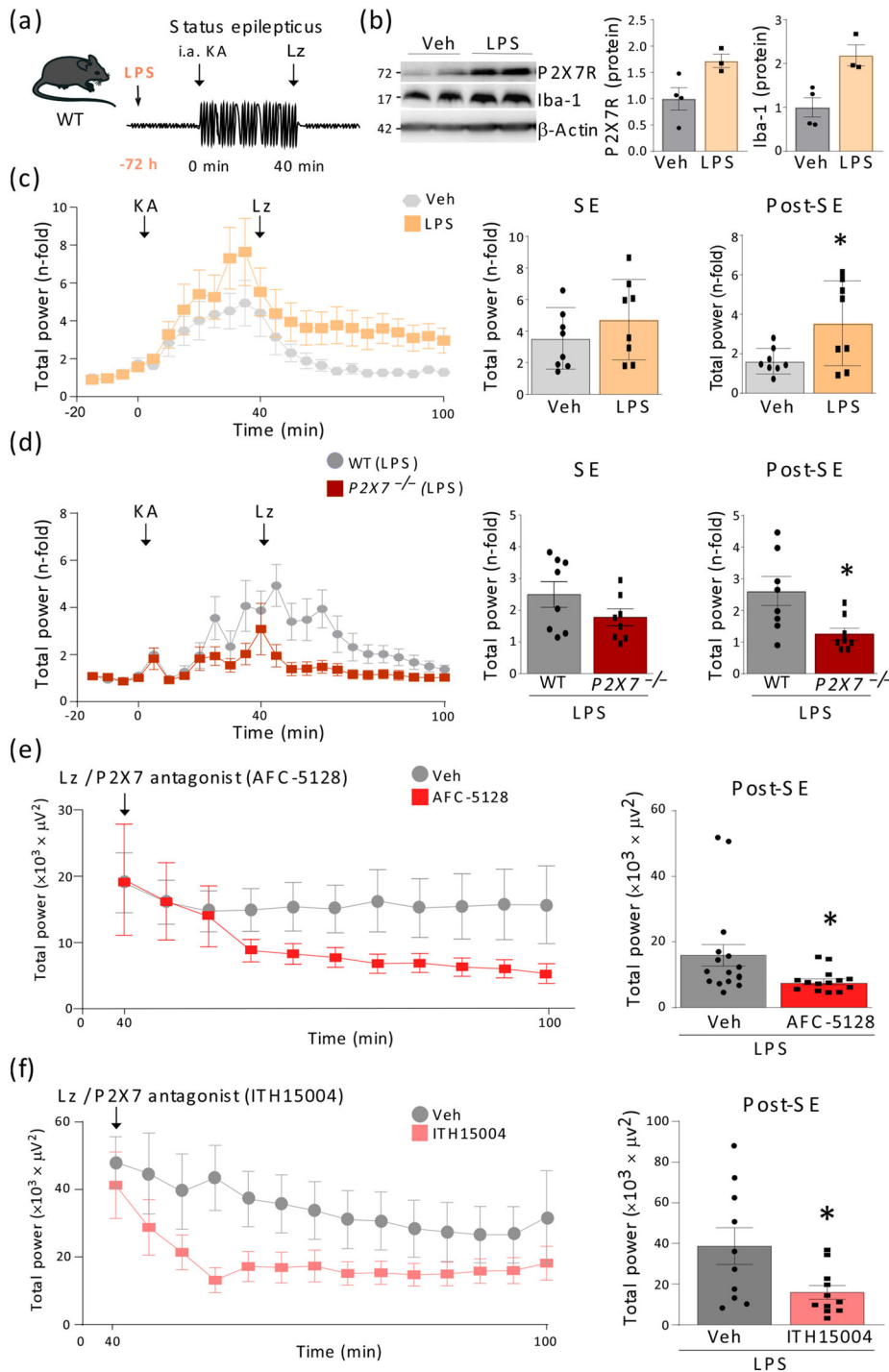


FIGURE 7 P2X7R deletion and antagonism in LPS-induced drug-refractoriness during status epilepticus. (a) Experimental design using lipopolysaccharide (LPS). Mice were treated with LPS ($1 \text{ mg} \cdot \text{kg}^{-1}$, i.p.) 72 h before intra-amygdala KA-induced status epilepticus (SE). (b) Representative Western blot ($n = 1$ per lane) using hippocampal tissue from vehicle (Veh) and LPS-injected mice and corresponding graphs on the right showing higher levels of P2X7 receptor and Iba-1 protein in mice treated with LPS, compared with vehicle treated mice (N = 4 [Veh] and 3 [LPS]). (c) No difference in EEG total power in LPS-treated mice during SE. Total power, however, was increased in LPS-treated mice, compared with vehicle-treated mice post-SE. Data shown are individual values with means \pm SEM; N = 8 per group. * $P < 0.05$, significantly different from Veh; unpaired Student's t test. (d) Graphs showing a significant reduction in the total power following status epilepticus in $P2X7^{-/-}$ mice, compared with WT mice. Data are shown as individual values with means \pm SEM; N = 8 per group. * $P < 0.05$ significantly different from WT; unpaired Student's t test. (e) Graphs showing a significant reduction in total power post-SE in mice treated with the P2X7 receptor antagonist AFC-5128 compared with vehicle-treated mice. Data shown are individual values with means \pm SEM; N = 15 per group. * $P < 0.05$ significantly different from WT; unpaired Student's t test. (f) Graphs showing a reduction in the total power post-status epilepticus in mice treated with the P2X7 receptor antagonist ITH15004, compared with mice treated with vehicle. Data shown are individual values with means \pm SEM; N = 11 per group. * $P < 0.05$, significantly different from Veh; unpaired Student's t test.

pathological process and ATP-enriched extracellular milieu for activation of P2X7 receptors in seizures and suggests that treatments based on these receptors might be more effective once pathological processes, such as inflammation, have been initiated.

Our findings that $P2X7^{-/-}$ mice responded better to treatment with lorazepam and that targeting of P2X7 receptors improves LPS-induced drug-refractoriness makes a strong case for the use of antagonists of these receptors, as adjuvant therapy in RSE. In line with

this, the combination of P2X7 receptor antagonists with the ASD carbamazepine, increased the seizure threshold in the maximal electroshock seizure test (Fischer et al., 2016) and intra-amygdala KA induced-status epilepticus (Engel et al., 2012). Whether P2X7 receptors contribute to drug-refractoriness during epilepsy remains to be determined. However, expression of P2X7 receptors was increased in hippocampi of drug-refractory epilepsy patients (Jimenez-Pacheco et al., 2016) and P2X7 receptor antagonists successfully reduced

severity (Amhaoul et al., 2016) and frequency (Jimenez-Pacheco et al., 2016) of seizures in epileptic mice and rats. Of note, mice, in which epilepsy was induced via intra-amygdala KA, were shown to be resistant to low doses of carbamazepine (Welzel et al., 2020).

How P2X7 receptors promote drug-refractoriness during status epilepticus remains to be established. Inflammatory processes induced by activated P2X7 receptors represent, however, a likely explanation. Expression of P2X7 receptors has repeatedly been shown to be increased in the brain post-status epilepticus (Engel et al., 2012; Jimenez-Pacheco et al., 2013) with the majority of studies suggesting a dominant up-regulation in microglia (Dona et al., 2009; Kaczmarek-Hajek et al., 2018). By using highly specific P2X7 receptor nanobodies (Danquah et al., 2016), we have shown that P2X7 receptor expression is increased in microglia as soon as 60 min post-KA injection, when mice show resistance to lorazepam (Engel et al., 2012), in line with early effects of P2X7 receptors being mediated via microglia activation. This is supported by the more activated microglia state that we observed in P2X7R-OE mice during status epilepticus and the fact that the anti-inflammatory drug minocycline restored normal responsiveness to anticonvulsants in these mice. We have previously shown a link between P2X7 receptor activation with seizures and inflammation by (a) demonstrating that P2X7 receptor blockade during status epilepticus decreased the release of IL-1 β in the hippocampus (Engel et al., 2012) and (b) treatment of epileptic mice with a P2X7 receptor antagonist reduced both astrocytosis and microgliosis (Jimenez-Pacheco et al., 2016). Interestingly, naïve P2X7R-OE mice showed an apparently normal microglia activation state, suggesting activation of P2X7 receptors occurred mainly under sustained pathological conditions. This could also explain why P2X7R-OE mice show a seizure burden similar to that in WT mice during the first 40 min following KA injection and that P2X7 receptor-dependent pro-inflammatory and resulting pro-convulsive responses only build up over time.

Our results suggest that P2X7 receptor-induced inflammatory responses are mainly mediated by microglial activation. We cannot, however, exclude the contribution of other cell types. While we did not find expression of P2X7 receptors in astrocytes here, these have also been shown to be activated by these receptors (Khan et al., 2019). Blockade of P2X7 receptors has further been shown to prevent astrocyte death following status epilepticus (Kim et al., 2009). Of note, while microglia had previously been ascribed a mainly pro-convulsant role, recent data also suggests a protective function of microglia with the depletion of microglia leading to a decreased seizure threshold (Badimon et al., 2020). This suggests that we must identify and target specific pro-convulsant pathways in microglia, rather than inhibiting global microglia function.

Which pathways are activated by P2X7 receptors in microglia during status epilepticus requires further investigation. An obvious explanation would be that pro-convulsive effects are mediated via increasing IL-1 β levels. IL-1 β reduced the anticonvulsant action of the benzodiazepine midazolam in primary murine cortical neuron cultures (Clarkson et al., 2017) and IL-1 receptor blockers such as **anakinra** protected the brain from damage induced by status epilepticus (Noe et al., 2013). An unexpected finding was, therefore, that genetic

ablation of different components of the NLRP3 inflammasome pathway led a seizure phenotype, similar to that in WT mice. This is in sharp contrast to previous studies, which reported that suppression of the NLRP3 inflammasome-caspase-1 axis provided neuroprotection and resulted in a milder epileptic phenotype (Meng et al., 2014; Shen et al., 2018; Vezzani et al., 2010). Differences in the specific animal models, the use of antagonists versus genetic models, different time-points of treatment and other factors may account for these opposing results. We demonstrated that, while antagonists of P2X7 receptors facilitated the effect of anticonvulsants, either genetic ablation or pharmacological inhibition of components of the NLRP3-caspase-1 signalling cascade had either no effect or even increased seizure severity. This not only suggests that blocking P2X7 receptors offers a better therapeutic strategy to treat status epilepticus compared with blockers of the NLRP3 pathway but also implies that P2X7 receptor signalling that causes drug unresponsiveness is independent of NLRP3 activation. Activation of the P2X7 receptors has been shown to activate several other cellular pathways, including those involving **ERK**, **Akt** and NF- κ B, that might contribute to inflammation and are activated following seizures or during epilepsy (Beamer et al., 2016; Vezzani et al., 2013). In addition, cathepsins, proteases which have been shown to contribute to IL-1 β maturation, have also been linked to signalling by P2X7 receptors (Lopez-Castejon et al., 2010). Nevertheless, independent of the specific mechanism, our data strongly suggest that the drug resistance induced by P2X7 receptor activation was mediated by microglia.

One limitation of our study is that we have not tested if mice remain resistant to treatment if treated with a combination of anticonvulsants. Also, anticonvulsants have only been used at a single dose. This needs to be addressed in future studies. Another limitation of our study is that we have used only one animal model. While the intra-amygdala KA model closely mimics the human condition, in terms of the neurodegeneration and lack of response to ASDs (Engel et al., 2012), our experiments should be replicated in status epilepticus models independent of KA. Finally, while P2X7 receptor-driven inflammation seems to be the most likely explanation for the effects of these receptors on responses to anticonvulsants, it is important to keep in mind that P2X7 receptors have been involved in numerous other pathological and also physiological mechanisms, including blood-brain barrier disruption, changes in neurotransmitter levels, synaptic reorganization, and neurogenesis (Sperlagh & Illes, 2014). For example, activation of neuronal P2X7 receptors modulates extracellular levels of the neurotransmitters GABA and glutamate and P2X7 receptor antagonists prevented the uptake of GABA more efficiently in tissue from epileptic patients, thereby potentially increasing GABAergic rundown (Barros-Barbosa et al., 2016).

In conclusion, we have, here, demonstrated that P2X7 receptors contribute to a diminished response to anticonvulsants during status epilepticus. This finding not only adds purinergic signalling as a potential neurotransmitter system involved in RSE generation but also provides strong evidence for the P2X7 receptor as a new drug target for RSE treatment. Importantly, P2X7 receptor antagonists are already in

clinical trials for non-epilepsy related CNS indications (Bhattacharya & Ceusters, 2020) which should accelerate development of P2X7 receptor-based treatments for status epilepticus and their application in the clinic. However, while very encouraging, future studies need to investigate the exact molecular mechanisms how activation of P2X7 receptors leads to a lack of response to anticonvulsants during status epilepticus. In addition, while the present study focuses on acute consequences (i.e., seizures, acute inflammation and neurodegeneration), follow-up studies should investigate whether suppression of P2X7 receptor signalling affects clinical outcomes, post-status epilepticus. In addition, it is important to investigate whether P2X7 receptor-based treatments can overcome drug-refractoriness also in epilepsy. This would extend the possible applications of P2X7 receptor antagonists to a much wider patient group where treatment remains a clinical challenge (Thijs et al., 2019).

ACKNOWLEDGEMENTS

This work was supported by funding from the Health Research Board HRA-POR-2015-1243, Science Foundation Ireland (13/SIRG/2098 and 17/CDA/4708, and co-funded under the European Regional Development Fund and by FutureNeuro industry partners 16/RC/3948), from the European Union's Horizon 2020 research and innovation programme under the Marie Skłodowska-Curie grant agreement (no. 766124 to T.E., A.N. and A.G.G.), from the H2020 Marie Skłodowska-Curie Actions Individual Fellowship (nos. 753527, 884956, 796600 and 840262), from the Irish Research Council (Government of Ireland Postdoctoral Fellowship Programme, GOIPD/2020/865 and GOIPD/2020/806), from the DFG (Project-ID 335447717 – SFB 1328 (P15) to A.N.), from FEDER/Ministerio de Ciencia, Innovación y Universidades – Agencia Estatal de Investigación (nos. SAF2017-88276-R and PID2020-116709RB-I00 to P.P.), from Fundación Séneca (nos. 20859/PI/18 and 21081/PDC/19 to P.P.), and from the European Research Council (ERC-2013-CoG grant 614578 and ERC-2019-PoC grant 899636 to P.P.). We thank Friedrich Koch-Nolte for providing the P2X7R-specific nanobody.

AUTHOR CONTRIBUTIONS

Conceptualization and methodology: E.B., J.M., M.A., T.E.; validation, formal analysis, investigation and data curation: E.B., J.M., M.A., A.M.M., G.M., G.C., L.G.-G., C.A.-V., J.S., B.Z., N.K.Y.N., S.M.; resources: T.E., M.H., K.D., P.P., D.C.H., A.N.; writing – original draft preparation: T.E., M.A.; writing – review and editing: all; supervision: T.E.; project administration: T.E.; funding acquisition: T.E., D.C.H., A.N., P.P., A.G.G. All authors have read and agreed to the published version of the manuscript.

CONFLICT OF INTEREST

The authors declare no conflicts of interest. The authors declare that this study received funding from FutureNeuro. However, the funder was not involved in the study design, collection, analysis, interpretation of data, the writing of this article or the decision to submit it for

publication. K.D. and M.H. are stakeholders in Lead Discovery Center GmbH and Affectis Pharmaceuticals, respectively, but had no influence in the study design.

DECLARATION OF TRANSPARENCY AND SCIENTIFIC RIGOUR

Declaration of transparency and scientific rigour This Declaration acknowledges that this paper adheres to the principles for transparent reporting and scientific rigour of preclinical research as stated in the *BJP* guidelines for [Design and Analysis](#), [Immunoblotting and Immunochemistry](#), and [Animal Experimentation](#), and as recommended by funding agencies, publishers and other organizations engaged with supporting research.

DATA AVAILABILITY STATEMENT

The data that support the findings of this study are available from the corresponding author upon reasonable request. Some data may not be made available because of privacy or ethical restrictions.

ORCID

Francesco Calzaferrì  <https://orcid.org/0000-0002-4781-2925>

Pablo Pelegrín  <https://orcid.org/0000-0002-9688-1804>

Annette Nicke  <https://orcid.org/0000-0001-6798-505X>

Tobias Engel  <https://orcid.org/0000-0001-9137-0637>

REFERENCES

- Alexander, S. P., Christopoulos, A., Davenport, A. P., Kelly, E., Mathie, A., Peters, J. A., Veale, E. L., Armstrong, J. F., Faccenda, E., Harding, S. D., Pawson, A. J., Southan, C., Davies, J. A., Abbracchio, M. P., Alexander, W., Al-hosaini, K., Bäck, M., Barnes, N. M., Bathgate, R., ... Ye, R. D. (2021). THE CONCISE GUIDE TO PHARMACOLOGY 2021/22: G protein-coupled receptors. *British Journal of Pharmacology*, 178(S1), S27–S156. <https://doi.org/10.1111/bph.15538>
- Alexander, S. P., Fabbro, D., Kelly, E., Mathie, A., Peters, J. A., Veale, E. L., Armstrong, J. F., Faccenda, E., Harding, S. D., Pawson, A. J., Southan, C., Davies, J. A., Beuve, A., Brouckaert, P., Bryant, C., Burnett, J. C., Farndale, R. W., Friebe, A., Garthwaite, J., ... Waldman, S. A. (2021). THE CONCISE GUIDE TO PHARMACOLOGY 2021/22: Catalytic receptors. *British Journal of Pharmacology*, 178(S1), S264–S312. <https://doi.org/10.1111/bph.15541>
- Alexander, S. P., Mathie, A., Peters, J. A., Veale, E. L., Striessnig, J., Kelly, E., Armstrong, J. F., Faccenda, E., Harding, S. D., Pawson, A. J., Southan, C., Davies, J. A., Aldrich, R. W., Attali, B., Baggetta, A. M., Becirovic, E., Biel, M., Bill, R. M., Catterall, W. A., ... Zhu, M. (2021). THE CONCISE GUIDE TO PHARMACOLOGY 2021/22: Ion channels. *British Journal of Pharmacology*, 178(S1), S157–S245. <https://doi.org/10.1111/bph.15539>
- Alves, M., De Diego Garcia, L., Conte, G., Jimenez-Mateos, E. M., D'Orsi, B., Sanz-Rodriguez, A., Prehn, J. H. M., Henshall, D. C., & Engel, T. (2019). Context-specific switch from anti- to pro-epileptogenic function of the P2Y1 receptor in experimental epilepsy. *The Journal of Neuroscience*, 39(27), 5377–5392. <https://doi.org/10.1523/JNEUROSCI.0089-19.2019>
- Amhaoul, H., Ali, I., Mola, M., Van Eetveldt, A., Szewczyk, K., Missault, S., Bielen, K., Kumar-Singh, S., Rech, J., Lord, B., Ceusters, M., Bhattacharya, A., & Dedeurwaerdere, S. (2016). P2X7 receptor antagonism reduces the severity of spontaneous seizures in a chronic model

- of temporal lobe epilepsy. *Neuropharmacology*, 105, 175–185. <https://doi.org/10.1016/j.neuropharm.2016.01.018>
- Badimon, A., Strasburger, H. J., Ayata, P., Chen, X., Nair, A., Ikegami, A., Hwang, P., Chan, A. T., Graves, S. M., Uweru, J. O., Ledderose, C., Kutlu, M. G., Wheeler, M. A., Kahan, A., Ishikawa, M., Wang, Y. C., Loh, Y. E., Jiang, J. X., Surmeier, D. J., ... Schaefer, A. (2020). Negative feedback control of neuronal activity by microglia. *Nature*, 586(7829), 417–423. <https://doi.org/10.1038/s41586-020-2777-8>
- Barros-Barbosa, A. R., Fonseca, A. L., Guerra-Gomes, S., Ferreira, F., Santos, A., Rangel, R., Lobo, M. G., Correia-de-Sá, P., & Cordeiro, J. M. (2016). Up-regulation of P2X7 receptor-mediated inhibition of GABA uptake by nerve terminals of the human epileptic neocortex. *Epilepsia*, 57(1), 99–110. <https://doi.org/10.1111/epi.13263>
- Beamer, E., Conte, G., & Engel, T. (2019). ATP release during seizures—A critical evaluation of the evidence. *Brain Research Bulletin*, 151, 65–73. <https://doi.org/10.1016/j.brainresbull.2018.12.021>
- Beamer, E., Goloncser, F., Horvath, G., Beko, K., Otrokocsi, L., Kovanyi, B., & Sperlagh, B. (2016). Purinergic mechanisms in neuroinflammation: An update from molecules to behavior. *Neuropharmacology*, 104, 94–104. <https://doi.org/10.1016/j.neuropharm.2015.09.019>
- Beamer, E., Kuchukulla, M., Boison, D., & Engel, T. (2021). ATP and adenosine—Two players in the control of seizures and epilepsy development. *Progress in Neurobiology*, 102105. <https://doi.org/10.1016/j.pneurobio.2021.102105>
- Bejtjemann, J. P., & Lowenstein, D. H. (2015). Status epilepticus in adults. *Lancet Neurology*, 14(6), 615–624. [https://doi.org/10.1016/S1474-4422\(15\)00042-3](https://doi.org/10.1016/S1474-4422(15)00042-3)
- Beutler, B., & Poltorak, A. (2000). The search for Lps: 1993-1998. *Journal of Endotoxin Research*, 6(4), 269–293. <https://doi.org/10.1177/09680519000060040401>
- Bhattacharya, A., & Ceusters, M. (2020). Targeting neuroinflammation with brain penetrant P2X7 antagonists as novel therapeutics for neuropsychiatric disorders. *Neuropsychopharmacology*, 45(1), 234–235. <https://doi.org/10.1038/s41386-019-0502-9>
- Calzaferri, F., Narros-Fernandez, P., de Pascual, R., de Diego, A. M. G., Nicke, A., Egea, J., García, A. G., & de Los Rios, C. (2021). Synthesis and pharmacological evaluation of novel non-nucleotide purine derivatives as P2X7 antagonists for the treatment of neuroinflammation. *Journal of Medicinal Chemistry*, 64(4), 2272–2290. <https://doi.org/10.1021/acs.jmedchem.0c02145>
- Clarkson, B. D. S., Kahoud, R. J., McCarthy, C. B., & Howe, C. L. (2017). Inflammatory cytokine-induced changes in neural network activity measured by waveform analysis of high-content calcium imaging in murine cortical neurons. *Scientific Reports*, 7(1), 9037. <https://doi.org/10.1038/s41598-017-09182-5>
- Conte, G., Nguyen, N. T., Alves, M., Diego-Garcia, L., Kenny, A., Nicke, A., Henshall, D. C., Jimenez-Mateos, E. M., & Engel, T. (2020). P2X7 receptor-dependent microRNA expression profile in the brain following status epilepticus in mice. *Frontiers in Molecular Neuroscience*, 13, 127. <https://doi.org/10.3389/fnmol.2020.00127>
- Crawshaw, A. A., & Cock, H. R. (2020). Medical management of status epilepticus: Emergency room to intensive care unit. *Seizure*, 75, 145–152. <https://doi.org/10.1016/j.seizure.2019.10.006>
- Danquah, W., Meyer-Schwesinger, C., Rissiek, B., Pinto, C., Serracant-Prat, A., Amadi, M., Iacenda, D., Knop, J. H., Hammel, A., Bergmann, P., Schwarz, N., Assunção, J., Rotthier, W., Haag, F., Tolosa, E., Bannas, P., Boué-Grabot, E., Magnus, T., Laeremans, T., ... Koch-Nolte, F. (2016). Nanobodies that block gating of the P2X7 ion channel ameliorate inflammation. *Science Translational Medicine*, 8(366), 366ra162. <https://doi.org/10.1126/scitranslmed.aaf8463>
- Davalos, D., Grutzendler, J., Yang, G., Kim, J. V., Zuo, Y., Jung, S., Littman, D. R., Dustin, M. L., & Gan, W. B. (2005). ATP mediates rapid microglial response to local brain injury in vivo. *Nature Neuroscience*, 8(6), 752–758. <https://doi.org/10.1038/nn1472>
- Di Virgilio, F., Dal Ben, D., Sarti, A. C., Giuliani, A. L., & Falzoni, S. (2017). The P2X7 receptor in infection and inflammation. *Immunity*, 47(1), 15–31. <https://doi.org/10.1016/j.immuni.2017.06.020>
- Diviney, M., Reynolds, J. P., & Henshall, D. C. (2015). Comparison of short-term effects of midazolam and lorazepam in the intra-amygdala kainic acid model of status epilepticus in mice. *Epilepsy & Behavior*, 51, 191–198. <https://doi.org/10.1016/j.yebeh.2015.07.038>
- Dona, F., Ulrich, H., Persike, D. S., Conceicao, I. M., Blini, J. P., Cavalheiro, E. A., & Fernandes, M. J. (2009). Alteration of purinergic P2X4 and P2X7 receptor expression in rats with temporal-lobe epilepsy induced by pilocarpine. *Epilepsy Research*, 83(2–3), 157–167. <https://doi.org/10.1016/j.eplepsyres.2008.10.008>
- Engel, T., Gomez-Villafuertes, R., Tanaka, K., Mesuret, G., Sanz-Rodriguez, A., Garcia-Huerta, P., Miras-Portugal, M. T., Henshall, D. C., & Diaz-Hernandez, M. (2012). Seizure suppression and neuroprotection by targeting the purinergic P2X7 receptor during status epilepticus in mice. *The FASEB Journal*, 26(4), 1616–1628. <https://doi.org/10.1096/fj.11-196089>
- Fischer, W., Franke, H., Krugel, U., Muller, H., Dinkel, K., Lord, B., Letavic, M. A., Henshall, D. C., & Engel, T. (2016). Critical evaluation of P2X7 receptor antagonists in selected seizure models. *PLoS ONE*, 11(6), e0156468. <https://doi.org/10.1371/journal.pone.0156468>
- Franke, H., Gunther, A., Grosche, J., Schmidt, R., Rossner, S., Reinhardt, R., Faber-Zuschratter, H., Schneider, D., & Illies, P. (2004). P2X7 receptor expression after ischemia in the cerebral cortex of rats. *Journal of Neuro-pathology and Experimental Neurology*, 63(7), 686–699. <https://doi.org/10.1093/jnen/63.7.686>
- Holmes, G. L. (2015). Cognitive impairment in epilepsy: The role of network abnormalities. *Epileptic Disorders*, 17(2), 101–116. <https://doi.org/10.1684/epd.2015.0739>
- Huang, K. F., Huang, W. T., Lin, K. C., Lin, M. T., & Chang, C. P. (2010). Interleukin-1 receptor antagonist inhibits the release of glutamate, hydroxyl radicals, and prostaglandin E(2) in the hypothalamus during pyrogen-induced fever in rabbits. *European Journal of Pharmacology*, 629(1–3), 125–131. <https://doi.org/10.1016/j.ejphar.2009.11.060>
- Jimenez-Mateos, E. M., Engel, T., Merino-Serrais, P., McKiernan, R. C., Tanaka, K., Mouri, G., Sano, T., O'tuathaigh, C., Waddington, J. L., Prenter, S., Delanty, N., Farrell, M. A., O'Brien, D. F., Conroy, R. M., Stallings, R. L., DeFelipe, J., & Henshall, D. C. (2012). Silencing microRNA-134 produces neuroprotective and prolonged seizure-suppressive effects. *Nature Medicine*, 18(7), 1087–1094. <https://doi.org/10.1038/nm.2834>
- Jimenez-Pacheco, A., Diaz-Hernandez, M., Arribas-Blazquez, M., Sanz-Rodriguez, A., Olivos-Ore, L. A., Artalejo, A. R., Alves, M., Letavic, M., Miras-Portugal, M. T., Conroy, R. M., Delanty, N., Farrell, M. A., O'Brien, D. F., Bhattacharya, A., Engel, T., & Henshall, D. C. (2016). Transient P2X7 receptor antagonism produces lasting reductions in spontaneous seizures and gliosis in experimental temporal lobe epilepsy. *The Journal of Neuroscience*, 36(22), 5920–5932. <https://doi.org/10.1523/JNEUROSCI.4009-15.2016>
- Jimenez-Pacheco, A., Mesuret, G., Sanz-Rodriguez, A., Tanaka, K., Mooney, C., Conroy, R., Miras-Portugal, M. T., Diaz-Hernandez, M., Henshall, D. C., & Engel, T. (2013). Increased neocortical expression of the P2X7 receptor after status epilepticus and anticonvulsant effect of P2X7 receptor antagonist A-438079. *Epilepsia*, 54(9), 1551–1561. <https://doi.org/10.1111/epi.12257>
- Kaczmarek-Hajek, K., Zhang, J., Kopp, R., Grosche, A., Rissiek, B., Saul, A., Bruzzone, S., Engel, T., Jooss, T., Krautloher, A., Tim Magnus, S. S., Stadelmann, C., Sirko, S., Koch-Nolte, F., Eulenburg, V., & Nicke, A. (2018). Re-evaluation of neuronal P2X7 expression using novel mouse models and a P2X7-specific nanobody. *eLife*, 7, e36217. <https://doi.org/10.7554/eLife.36217>

- Khan, M. T., Deussing, J., Tang, Y., & Illes, P. (2019). Astrocytic rather than neuronal P2X7 receptors modulate the function of the tri-synaptic network in the rodent hippocampus. *Brain Research Bulletin*, 151, 164–173. <https://doi.org/10.1016/j.brainresbull.2018.07.016>
- Kim, J. E., & Kang, T. C. (2011). The P2X7 receptor-pannexin-1 complex decreases muscarinic acetylcholine receptor-mediated seizure susceptibility in mice. *The Journal of Clinical Investigation*, 121(5), 2037–2047. <https://doi.org/10.1172/JCI44818>
- Kim, J. E., Kwak, S. E., Jo, S. M., & Kang, T. C. (2009). Blockade of P2X receptor prevents astroglial death in the dentate gyrus following pilocarpine-induced status epilepticus. *Neurological Research*, 31(9), 982–988. <https://doi.org/10.1179/174313209X389811>
- Kobayashi, K., Imagama, S., Ohgomori, T., Hirano, K., Uchimura, K., Sakamoto, K., Hirakawa, A., Takeuchi, H., Suzumura, A., Ishiguro, N., & Kadomatsu, K. (2013). Minocycline selectively inhibits M1 polarization of microglia. *Cell Death & Disease*, 4, e525. <https://doi.org/10.1038/cddis.2013.54>
- Lilley, E., Stanford, S. C., Kendall, D. E., Alexander, S. P. H., Cirino, G., Docherty, J. R., George, C. H., Insel, P. A., Izzo, A. A., Ji, Y., Panettieri, R. A., Sobey, C. G., Stefanska, B., Stephens, G., Teixeira, M., & Ahluwalia, A. (2020). ARRIVE 2.0 and the British Journal of Pharmacology: Updated guidance for 2020. *British Journal of Pharmacology*, 177(16), 3611–3616. <https://doi.org/10.1111/bph.15178>
- Liu, X., Zhao, Z., Ji, R., Zhu, J., Sui, Q. Q., Knight, G. E., Burnstock, G., He, C., Yuan, H., & Xiang, Z. (2017). Inhibition of P2X7 receptors improves outcomes after traumatic brain injury in rats. *Purinergic Signal*, 13(4), 529–544. <https://doi.org/10.1007/s11302-017-9579-y>
- Lopez-Castejon, G., Theaker, J., Pelegrin, P., Clifton, A. D., Braddock, M., & Surprenant, A. (2010). P2X(7) receptor-mediated release of cathepsins from macrophages is a cytokine-independent mechanism potentially involved in joint diseases. *Journal of Immunology*, 185(4), 2611–2619. <https://doi.org/10.4049/jimmunol.1000436>
- Loscher, W. (2007). The pharmacokinetics of antiepileptic drugs in rats: Consequences for maintaining effective drug levels during prolonged drug administration in rat models of epilepsy. *Epilepsia*, 48(7), 1245–1258. <https://doi.org/10.1111/j.1528-1167.2007.01093.x>
- Loscher, W. (2017). Animal models of seizures and epilepsy: Past, present, and future role for the discovery of antiseizure drugs. *Neurochemical Research*, 42(7), 1873–1888. <https://doi.org/10.1007/s11064-017-2222-z>
- Mayer, S. A., Claassen, J., Lokin, J., Mendelsohn, F., Dennis, L. J., & Fitzsimmons, B. F. (2002). Refractory status epilepticus: Frequency, risk factors, and impact on outcome. *Archives of Neurology*, 59(2), 205–210. <https://doi.org/10.1001/archneur.59.2.205>
- Meng, X. F., Tan, L., Tan, M. S., Jiang, T., Tan, C. C., Li, M. M., Wang, H. F., & Yu, J. T. (2014). Inhibition of the NLRP3 inflammasome provides neuroprotection in rats following amygdala kindling-induced status epilepticus. *Journal of Neuroinflammation*, 11, 212. <https://doi.org/10.1186/s12974-014-0212-5>
- Monif, M., Reid, C. A., Powell, K. L., Smart, M. L., & Williams, D. A. (2009). The P2X7 receptor drives microglial activation and proliferation: A trophic role for P2X7R pore. *The Journal of Neuroscience*, 29(12), 3781–3791. <https://doi.org/10.1523/JNEUROSCI.5512-08.2009>
- Morris, G., Jiruska, P., Jefferys, J. G., & Powell, A. D. (2016). A new approach of modified submerged patch clamp recording reveals interneuronal dynamics during epileptiform oscillations. *Frontiers in Neuroscience*, 10, 519. <https://doi.org/10.3389/fnins.2016.00519>
- Mouri, G., Jimenez-Mateos, E., Engel, T., Dunleavy, M., Hatazaki, S., Paucard, A., Matsushima, S., Taki, W., & Henshall, D. C. (2008). Unilateral hippocampal CA3-predominant damage and short latency epileptogenesis after intra-amygdala microinjection of kainic acid in mice. *Brain Research*, 1213, 140–151. <https://doi.org/10.1016/j.brainres.2008.03.061>
- Nieoczym, D., Socala, K., & Wlaz, P. (2017). Evaluation of the anticonvulsant effect of brilliant blue G, a selective P2X7 receptor antagonist, in the iv PTZ-, maximal electroshock-, and 6 Hz-induced seizure tests in mice. *Neurochemical Research*, 42(11), 3114–3124. <https://doi.org/10.1007/s11064-017-2348-z>
- Noe, F. M., Polascheck, N., Frigerio, F., Bankstahl, M., Ravizza, T., Marchini, S., Beltrame, L., Banderó, C. R., Löscher, W., & Vezzani, A. (2013). Pharmacological blockade of IL-1beta/IL-1 receptor type 1 axis during epileptogenesis provides neuroprotection in two rat models of temporal lobe epilepsy. *Neurobiology of Disease*, 59, 183–193. <https://doi.org/10.1016/j.nbd.2013.07.015>
- Pelegrin, P. (2021). P2X7 receptor and the NLRP3 inflammasome: Partners in crime. *Biochemical Pharmacology*, 187, 114385. <https://doi.org/10.1016/j.bcp.2020.114385>
- Percie du Sert, N., Hurst, V., Ahluwalia, A., Alam, S., Avey, M. T., Baker, M., Browne, W. J., Clark, A., Cuthill, I. C., Dirnagl, U., Emerson, M., Garner, P., Holgate, S. T., Howells, D. W., Karp, N. A., Lazic, S. E., Lidster, K., MacCallum, C. J., Macleod, M., ... Würbel, H. (2020). The ARRIVE guidelines 2.0: Updated guidelines for reporting animal research. *BMC Veterinary Research*, 16(1), 242. <https://doi.org/10.1186/s12917-020-02451-y>
- Rossi, S., Furlan, R., De Chiara, V., Motta, C., Studer, V., Mori, F., Musella, A., Bergami, A., Muzio, L., Bernardi, G., Battistini, L., Martino, G., & Centonze, D. (2012). Interleukin-1beta causes synaptic hyperexcitability in multiple sclerosis. *Annals of Neurology*, 71(1), 76–83. <https://doi.org/10.1002/ana.22512>
- Sanchez, S., & Rincon, F. (2016). Status epilepticus: Epidemiology and public health needs. *Journal of Clinical Medicine*, 5(8), 71. <https://doi.org/10.3390/jcm5080071>
- Sebastian-Serrano, A., Engel, T., de Diego-Garcia, L., Olivos-Ore, L. A., Arribas-Blazquez, M., Martinez-Frailes, C., Pérez-Díaz, C., Millán, J. L., Artalejo, A. R., Miras-Portugal, M. T., Henshall, D. C., & Diaz-Hernandez, M. (2016). Neurodevelopmental alterations and seizures developed by mouse model of infantile hypophosphatasia are associated with purinergic signalling deregulation. *Human Molecular Genetics*, 25(19), 4143–4156. <https://doi.org/10.1093/hmg/ddw248>
- Shen, K., Mao, Q., Yin, X., Zhang, C., Jin, Y., Deng, A., Gu, Z., & Chen, B. (2018). NLRP3 inflammasome activation leads to epileptic neuronal apoptosis. *Current Neurovascular Research*, 15(4), 276–281. <https://doi.org/10.2174/1567202616666181122165540>
- Sperlagh, B., & Illes, P. (2014). P2X7 receptor: An emerging target in central nervous system diseases. *Trends in Pharmacological Sciences*, 35(10), 537–547. <https://doi.org/10.1016/j.tips.2014.08.002>
- Surprenant, A., Rassendren, F., Kawashima, E., North, R. A., & Buell, G. (1996). The cytolytic P2Z receptor for extracellular ATP identified as a P2X receptor (P2X7). *Science*, 272(5262), 735–738. <https://doi.org/10.1126/science.272.5262.735>
- Thijs, R. D., Surges, R., O'Brien, T. J., & Sander, J. W. (2019). Epilepsy in adults. *Lancet*, 393(10172), 689–701. [https://doi.org/10.1016/S0140-6736\(18\)32596-0](https://doi.org/10.1016/S0140-6736(18)32596-0)
- Twele, F., Tollner, K., Bankstahl, M., & Loscher, W. (2016). The effects of carbamazepine in the intrahippocampal kainate model of temporal lobe epilepsy depend on seizure definition and mouse strain. *Epilepsia Open*, 1(1–2), 45–60. <https://doi.org/10.1002/epi4.2>
- Vezzani, A., Aronica, E., Mazarati, A., & Pittman, Q. J. (2013). Epilepsy and brain inflammation. *Experimental Neurology*, 244, 11–21. <https://doi.org/10.1016/j.expneurol.2011.09.033>
- Vezzani, A., Balosso, S., Maroso, M., Zardoni, D., Noe, F., & Ravizza, T. (2010). ICE/caspase 1 inhibitors and IL-1beta receptor antagonists as

- potential therapeutics in epilepsy. *Current Opinion in Investigational Drugs*, 11(1), 43–50.
- Vezzani, A., Dingledine, R., & Rossetti, A. O. (2015). Immunity and inflammation in status epilepticus and its sequelae: Possibilities for therapeutic application. *Expert Review of Neurotherapeutics*, 15(9), 1081–1092. <https://doi.org/10.1586/14737175.2015.1079130>
- Vezzani, A., French, J., Bartfai, T., & Baram, T. Z. (2011). The role of inflammation in epilepsy. *Nature Reviews. Neurology*, 7(1), 31–40. <https://doi.org/10.1038/nrneuro.2010.178>
- Vezzani, A., & Viviani, B. (2015). Neuromodulatory properties of inflammatory cytokines and their impact on neuronal excitability. *Neuropharmacology*, 96(Pt A), 70–82. <https://doi.org/10.1016/j.neuropharm.2014.10.027>
- Welzel, L., Schidlitzki, A., Twele, F., Anjum, M., & Loscher, W. (2020). A face-to-face comparison of the intra-amygdala and intrahippocampal kainate mouse models of mesial temporal lobe epilepsy and their utility for testing novel therapies. *Epilepsia*, 61(1), 157–170. <https://doi.org/10.1111/epi.16406>

SUPPORTING INFORMATION

Additional supporting information may be found in the online version of the article at the publisher's website.

How to cite this article: Beamer, E., Morgan, J., Alves, M., Menéndez Méndez, A., Morris, G., Zimmer, B., Conte, G., de Diego-García, L., Alarcón-Vila, C., Yiu Ng, N. K., Madden, S., Calzaferri, F., de los Ríos, C., García, A. G., Hamacher, M., Dinkel, K., Pelegrín, P., Henshall, D. C., Nicke, A., & Engel, T. (2022). Increased expression of the ATP-gated P2X7 receptor reduces responsiveness to anti-convulsants during status epilepticus in mice. *British Journal of Pharmacology*, 1–21. <https://doi.org/10.1111/bph.15785>